

Article

Thermodynamic Geometry and Topological Einstein–Yang–Mills Black Holes

Stefano Bellucci * and Bhupendra Nath Tiwari

INFN-Laboratori Nazionali di Frascati, Via E. Fermi 40, 00044 Frascati, Italy;

E-Mail: bntiwari.iitk@gmail.com

* Author to whom correspondence should be addressed; E-Mail: bellucci.stefano@lnf.infn.it;
Tel.: +39-06-94032888; +39-06-94038222; Fax: +39-06-94032716.

Received: 25 April 2012; in revised form: 8 June 2012 / Accepted: 11 June 2012 /

Published: 13 June 2012

Abstract: From the perspective of the statistical fluctuation theory, we explore the role of the thermodynamic geometries and vacuum (in)stability properties for the topological Einstein–Yang–Mills black holes. In this paper, from the perspective of the state-space surface and chemical Weinhold surface of higher dimensional gravity, we provide the criteria for the local and global statistical stability of an ensemble of topological Einstein–Yang–Mills black holes in arbitrary spacetime dimensions $D \geq 5$. Finally, as per the formulations of the thermodynamic geometry, we offer a parametric account of the statistical consequences in both the local and global fluctuation regimes of the topological extremal Einstein–Yang–Mills black holes.

Keywords: thermodynamic geometry; topological Einstein–Yang–Mills black holes; higher dimensional gravity; cosmological constant

1. Introduction

Thermodynamic geometry [1–26] plays important role in understanding the stability and phase structure properties of black holes. There have been several investigations made in this direction, which explore the thermodynamic structures of black holes in general relativity, string theory and M-theory. In this paper, we examine thermodynamic structures of topological Einstein–Yang–Mills black holes.

From the perspective of the $SU(2)$ gauge theory, we explore the thermodynamic properties of the black hole solutions in non-Abelian gauge theory. In particular, the present consideration investigates the thermodynamic stability structures of a class of two parameter extremal black hole configurations which carry an electric charge e and the cosmological constant $\Lambda := kn(n-1)/l^2$, where l is the curvature of the Anti-de Sitter (AdS) space. Here, for a given $(n+1)$ -dimensional topological Einstein–Yang–Mills black hole, the symbol k takes values over the set $\{-1, 1\}$ respectively for the asymptotically AdS and de Sitter (dS) solutions. From the perspective of the $SU(2)$ gauge theory, [27] offers the subject matter, namely, the solitonic features towards such a consideration. In this concern, the work of Yasskin [28] gives the corresponding colored black hole solutions with $SO(3)$ gauge group symmetry.

For a given colored black hole solution, in the above setup, the black hole uniqueness theorem leads to the fact that arbitrary dimensional topological solutions of the Einstein–Yang–Mills black holes are hairy in their character. In contrast to the Kerr–Newman family, the exterior geometry of the both the above family of solutions, apart from the global asymptotic charges, require additional parameters of the metric tensor and the corresponding matter fields [29–31]. The nature of these solutions have been extended for the higher derivative corrections. Namely, [32,33] provide the contribution arising from the Gauss–Bonnet terms. [34–38] describe the corresponding cosmological constant contributions to the entropy and ADM mass of the topological Einstein–Yang–Mills black holes. It is worth mentioning further that all the above solutions indicate a non-trivial domain of instability for the non-negative cosmological constant solutions, see for a reference [39]. [37,40] provide the (in)stability structures of the associated negative cosmological constant black holes.

From the perspective of gauge field theories, for a given N -parameter semi-simple Lie gauge group, the action of $(n+1)$ -dimensional Einstein–Yang–Mills gravity theory describes black hole solutions. This consideration involves three types of contributions to the Lagrangian of the theory. These terms are respectively the contributions arising from the Ricci scalar, cosmological constant (or AdS curvature) and the Yang–Mills field strength tensor. The equations of the motion of such a Lagrangian are obtained via variations of the background space-time metric tensor and the underlying Yang–Mills gauge fields. For given gauge fields and space-time metric tensor, the equations of motion render as a set of coupled Yang–Mills equations with sources and the Einstein field equations with cosmological constant. Such a theory can be simplified via the consideration of the Cartan’s criteria. Namely, this yields to the fact that both the energy momentum tensor and current of the theory can be expressed in terms of the structure constants of the gauge group, gauge coupling constants and underlying gauge fields. From the consideration of Wu–Yang Ansatz [41,42] provides explicit topological character of Einstein–Yang–Mills black holes and thus one obtains black hole solutions in four, five and arbitrary space-time dimensions. It is worth mentioning that the determination of the currents and the gauge fields of the theory requires specification of structure constants of the gauge group. Moreover, the static space-time metric tensor of such a black hole, which possesses the hyperbolic horizon, arises by solving the corresponding cosmological Einstein field equations for specific components of the background space-time metric tensor. In this perspective, [43] provides a class of static non-Abelian five-dimensional black holes in the theory of $\mathcal{N} = 8$ maximal gauged supergravity.

Notice further that the [42] provides an appropriate platform to study the thermodynamic geometric properties of the non-Abelian black holes. In any case, as a generalization of the Abelian

Einstein–Maxwell gravity, these black holes are based on the analysis of the Einstein field equations. For nonlinear field sources with generic topological nature, we shall offer exact thermodynamical properties of the standard four and higher dimensional black holes in the theory of the Yang–Mills gravity. Specifically, for given $(n + 1)$ -dimensional topological Einstein–Yang–Mills black holes with a negative cosmological constant, the thermodynamics lies on the properties of the Einstein field equations, gauge current and stress-energy tensor for arbitrary finite semi-simple gauge group. In fact, the consideration of [42] leads to explicit horizon properties of the four dimensional solution with $SO(2, 1)$ gauge symmetry. The above research direction further continues towards the topological properties of a family of logarithmically corrected black hole solutions in the five and other higher dimensional generalizations. The examination of the five-dimensional static black holes provides interesting issues for the hyperbolic horizon spherically symmetric solutions with $SO(3, 1)$ gauge isometries. In this perspective, we refer the reader to [42] for explicit expressions of the mass, entropy and Hawking temperature of the black holes of the present interest. Namely, the consideration of the thermodynamic geometry offers further issues for the non-static asymptotically de Sitter solutions in six and higher space-time dimensional Einstein–Yang–Mills gravity with a non-negative mass, which we relegate to the section 3 and 4 of this paper. The motivation of the present paper lies in the fact that these solutions describe black holes if the corresponding solutions exist in the Einstein–Maxwell gravity [42]. Namely, it is worth mentioning that the notion of the thermodynamic geometry opens new direction to examine the stability properties of topological Einstein–Yang–Mills black holes in arbitrary $(n + 1)$ -dimensional space-time with $SO(n(n - 1)/2 - 1, 1)$ semi-simple gauge group symmetries.

Here, our goal is to analyze the statistical nature of the topological Einstein–Yang–Mills black holes, in general. Namely, we wish to explicate the local and global statistical stability of an ensemble of such black holes in arbitrary space-time dimensions $D \geq 5$. Our framework allows one to geometrically explore the nature of the local and global statistical correlations about a fixed vacuum of the non-Abelian Yang–Mills gauge theory containing Einstein–Yang–Mills black holes. As per the quantitative analysis of the thermodynamic geometric model provided in the section 2, this paper offers an explicit realization of the statistical (in)stabilities. For the given black hole entropy and mass, we shall illustrate that the parametric fluctuations are intrinsic geometric in the nature. Subsequently, the framework of fluctuation theory is capable of offering an appropriate account of the statistical properties of all finite dimensional topological Einstein–Yang–Mills black hole configurations. From the perspective of the thermodynamic geometries and fluctuation theory, the statistical ensemble (in)stabilities via the Ruppeiner geometry and the corresponding Legendre transformed Weinhold geometry of the arbitrary finite space-time dimensional topological Einstein–Yang–Mills black hole configurations are of the particular interest in the consideration of the present paper.

The rest of the paper is organized as follow. In Section 2, we provide a brief review of the fluctuation theory of the two parameter black hole configuration and thereby specialize it from the perspective application of the thermodynamic Riemannian geometries. In Section 3, we analyze the Ruppeiner geometry for the five dimensional topological Einstein–Yang–Mills black hole configuration and thereby extend our consideration for the ensemble of arbitrary finite dimensional topological Einstein–Yang–Mills black holes. In Section 4, we explore the above consideration from the perspective of the Weinhold geometry, where we first analyze the ensemble of the five dimensional topological

Einstein–Yang–Mills black holes and subsequently consider the case of arbitrary finite dimensional topological Einstein–Yang–Mills black hole configuration. Finally, in Section 5, we present our conclusions and some remarks for a future investigation such as the corresponding non-extremal configurations.

2. Thermodynamic Geometry

In what follows next that we consider the Riemannian geometric model whose covariant metric tensor may be defined as the Hessian matrix of the entropy with respect to an arbitrary number of parameters characterizing a black hole system of the statistical interest. We shall examine the nature of the fluctuation properties with a minimal number of parameters, such as fixed volume system, characterizing the thermodynamics of the associated equilibrium statistical configuration of an ensemble of arbitrary finite dimensional topological Einstein–Yang–Mills black holes. In particular, let us define the entropy representation of the chosen black hole configuration with the entropy $S(x_i)$ for a given set of parameters of the configuration. Such a definition can be introduced in terms of the parameters, such as the entropy S , temperature T , mass M , charges q_i , and others if any, of the black hole. This gives a finite dimensional basis set $\{x_i\}$ of the black hole fluctuations over a given statistical equilibrium ensemble.

As mentioned above, in the present work we only consider extremal black holes. However, let us notice immediately that the issue of stability we study for the extremal case, which concerns fluctuations of the cosmological constant instead of the temperature (which is considered fixed at zero value), is based upon a method that can be applied also to the case of black holes with non-vanishing temperature, which lies beyond the scope of the present paper and can be considered in a separate publication. We also stress that it is our primary focus in the present consideration, to study an ensemble of topological Einstein–Yang–Mills black holes described in terms of the electrical charge, entropy, mass, and cosmological constant, which is then considered as one of the fluctuating parameters. The following analysis, carried out in the section below, allows us to consider issues of stability of different black holes, living in universes having different cosmological constant.

Herewith, for a given ensemble of topological Einstein–Yang–Mills black holes described in terms of a set of parameters x_i such as the electrical charge e , entropy S , mass M , and cosmological constant λ as statistical events $\{i_j \mid j \in \Lambda\} \subset Z$ on a finite set Λ as a finite lattice, the Gaussian distribution function can be determined the fluctuation of $\{x_i\}$ over an equilibrium black hole configuration. Thus, as per the theory of general coordinate transformations of a differentiable manifold, we shall consider the state-space and chemical surfaces parameterized by $\{l, e\}$. Physically, in the sense of fluid/ gravity correspondence [44] relating the dynamics of Einstein’s equations with a given non-zero cosmological constant to the dynamics of relativistic fluid equations, we shall view the flow of the entropy S and mass M of the black hole in terms of its parameters $\{l, e\}$. Over such a given equilibrium configuration [45], the fluctuation theory provides the underlying Riemannian geometric inner product structures, see for a review [1].

Moreover, by considering the extremal limit of a given non-extremal black hole system, we examine the stability of an extremal ensemble of topological Einstein–Yang–Mills black holes for the limiting zero temperature configurations. The Weinhold geometry can be realized as the fluctuations of the chemical potentials. The corresponding Legendra transformed Ruppeiner geometry is realized when

the charge and cosmological constant are allowed to fluctuate [1]. It is worth mentioning that the method of the fluctuation theory as invoked here applies to the non-extremal configurations, as well. Indeed, as outlined above, the stability analysis of the corresponding non-extremal topological black hole ensemble, involves fluctuations in all of the concerned black hole parameters. Namely, for the non-extremal topological Einstein–Yang–Mills black holes, our consideration opens the three parameter generalization for a perspective research.

In this setup, the set $\{x_i\}$, for $i = 1, \dots, n$, when treated as a set of extensive thermodynamic variables, forms coordinate charts for the corresponding intrinsic manifold. In this sense, an appropriate choice of the parameters x_i characterizes the entropy of the system. This characterization of the fluctuations of an ensemble of finite dimensional topological Einstein–Yang–Mills black holes renders into the so-called Ruppeiner geometry [1–6]. In general, the components of the covariant Ruppeiner metric tensor are defined as

$$g_{ij} := -\frac{\partial^2 S(\vec{x})}{\partial x^i \partial x^j} \quad (1)$$

where the vector $\vec{x} = (x^i) \in M_n$. Explicitly, for the case of the two-dimensional intrinsic Riemannian geometry parameterized by $\vec{x} = (x_1, x_2) \in M_2$, the components of the thermodynamic Ruppeiner metric tensor are given by

$$\begin{aligned} g_{x_1 x_1} &= -\frac{\partial^2 S}{\partial x_1^2} \\ g_{x_1 x_2} &= -\frac{\partial^2 S}{\partial x_1 \partial x_2} \\ g_{x_2 x_2} &= -\frac{\partial^2 S}{\partial x_2^2} \end{aligned} \quad (2)$$

Notice that the components of the intrinsic metric tensor are associated to the respective pair correlation functions of the concerned entropy flow. It is worth mentioning that the co-ordinates of the underlying fluctuations lie on the surface of the parameters $\{x_1, x_2\}$, which in the statistical sense, gives the origin of the fluctuations in the vacuum topological Einstein–Yang–Mills black holes. This is because the components of the Ruppeiner metric tensor comprise the Gaussian fluctuations of the degeneracy of the microstates, which is a function of the parameters of the associated macroscopic black hole configuration. For a given black hole, the local stability of the underlying statistical system requires both the principle components to be positive. In this concern, the diagonal components of the Ruppeiner metric tensor, $\{g_{x_i x_i} \mid i = 1, 2\}$ signify the heat capacities of the chosen system. From the perspective of the fluctuation theory, it is required that the diagonal components of the Ruppeiner metric tensor remain positive definite quantities, *viz.* we must have

$$g_{x_i x_i} > 0, \quad i = 1, 2 \quad (3)$$

for the existence of the local statistical stability of the two parameter black holes. In this case, we see that the determinant of the metric tensor can be given as

$$\|g\| = S_{x_1 x_1} S_{x_2 x_2} - S_{x_1 x_2}^2 \quad (4)$$

Notice further that the global stability of a given black hole ensemble requires the positivity of the $\|g\|$, in addition to the positivity of the diagonal components of the Ruppeiner metric tensor. The Christoffel connections Γ_{ijk} , Riemann curvature tensors R_{ijkl} , Ricci tensors R_{ij} and the scalar curvature R of the two dimensional thermodynamic geometry (M_2, g) can be computed further. With the above notion, we find that the scalar curvature can be shown to be

$$R = \frac{1}{2\|g\|^2} \left(S_{x_2x_2}S_{x_1x_1x_1}S_{x_1x_2x_2} + S_{x_1x_2}S_{x_1x_1x_2}S_{x_1x_2x_2} + S_{x_1x_1}S_{x_1x_1x_2}S_{x_2x_2x_2} - S_{x_1x_2}S_{x_1x_1x_1}S_{x_2x_2x_2} - S_{x_1x_1}S_{x_1x_2x_2}^2 - S_{x_2x_2}S_{x_1x_1x_2}^2 \right) \tag{5}$$

Interestingly, the relation between the thermodynamic scalar curvature and the Riemann curvature tensor for any two dimensional intrinsic Riemannian geometry is given (see for details [8,9]) by

$$R = \frac{2}{\|g\|} R_{x_1x_2x_1x_2} \tag{6}$$

It is worth mentioning that the relationship of a non-zero scalar curvature with an underlying interacting statistical system remains valid for higher dimensional intrinsic manifolds as well. Namely, the connection of a divergent (scalar) curvature with phase transitions can be analyzed from the Hessian matrix of the considered fluctuating entropy. In the sense of the state-space fluctuations, such a consideration of the statistical fluctuations requires an ensemble of vacuum black hole configurations. Specifically, the present article divulges the underlying geometric description in the Gaussian approximation. Such an analysis is thus concerned in the neighborhood of the small probability fluctuations. Hereby, the present consideration takes into account the scales that are larger than the correlation length of the system, in which a few microstates do not dominate the entire macroscopic phase-space configuration of the chosen dimensional topological Einstein–Yang–Mills black hole ensemble.

As per the Gaussian distribution theory, the thermodynamic Ruppeiner metric may be expressed as the second moment of the quadratic fluctuations or the statistical parametric pair correlation functions. Indeed, an explicit evaluation shows the components of the inverse metric tensor are

$$g^{ij} = \langle x^i | x^j \rangle \tag{7}$$

where $\{x_i\}$'s are the extensive thermodynamic variables conjugate to the intensive variables $\{X_i\}$. Moreover, such Riemannian structures may also be expressed in terms of a suitable thermodynamic potential obtained by a Legendre transformation. In Section 4, we explicate such a consideration for the Weinhold geometry, arising from the fluctuations of the mass of the topological Einstein–Yang–Mills black hole in space-time dimensions $D \geq 5$. For a given statistical ensemble, it is worth mentioning that the above intrinsic geometric setup corresponds to certain general coordinate transformations on the space of equilibrium states.

3. Ruppeiner Geometry

In this section, we examine thermodynamic fluctuation properties of the topological Einstein–Yang–Mills black hole as per the prescription of the thermodynamic Ruppeiner geometry.

Following the explanations in the previous section, we first consider the analysis of the vacuum statistical correlation for an ensemble of five dimensional topological Einstein–Yang–Mills black hole. For the given vacuum parameters, we shall exhibit that the parametric thermodynamic geometry is well capable to describe the perspective statistical (in)stability corresponding to the topological Einstein–Yang–Mills black hole configurations. Subsequently, we analyze the above properties for an ensemble of arbitrary space-time dimensional topological Einstein–Yang–Mills black holes.

3.1. Five Dimensional Black Holes

From the [42], the entropy of a topological Einstein–Yang–Mills black hole in space-time dimension $D = 5$ can be expressed as

$$S(l, e) := \frac{1}{32} V_3 l^3 \left(1 + \sqrt{1 + \frac{8e^2}{l^2}}\right)^3 \tag{8}$$

As per the notion of the Gaussian fluctuation theory, we see that the line elements associated with the Ruppeiner geometry is given by

$$ds^2 = -\left(\frac{\partial^2}{\partial e^2} S(l, e)\right) de^2 - 2\left(\frac{\partial^2}{\partial l \partial e} S(l, e)\right) de dl - \left(\frac{\partial^2}{\partial l^2} S(l, e)\right) dl^2 \tag{9}$$

Before proceeding further, we introduce the following scaling factor

$$f := \sqrt{\frac{l^2 + 8e^2}{l^2}} \tag{10}$$

With this convention, we find the following components of the Ruppeiner metric tensor

$$\begin{aligned} g_{uu} &= -\frac{3}{8} V_3 \frac{(6e^2 f + 10e^2 + l^2 f + l^2) l (1 + f)}{f (l^2 + 8e^2)} \\ g_{el} &= -\frac{3}{4} V_3 \frac{(16e^2 + l^2 + l^2 f) e (1 + f)}{f (l^2 + 8e^2)} \\ g_{ee} &= -\frac{3}{4} V_3 \frac{l (16e^2 f + l^2 + l^2 f) (1 + f)}{f (l^2 + 8e^2)} \end{aligned} \tag{11}$$

For a given V_3 , in order to analyze the instability occurring due to a entropy fluctuations with respect to the electric charge e and cosmological constant parameter l , Figures 1 and 2 show the fluctuations in the diagonal components $\{g_{ee}, g_{uu}\}$ of the metric tensor. The value of V_3 depends on the phase-space of the black hole, and thus it may vary from vacuum to vacuum, however the procedure of the state-space analysis remains the same. In the regime of $l \in (-1, 1)$ and $e \in (0, 10)$, we notice that the amplitude of $\{g_{ee}\}$ takes a value between $\{-40, +40\}$. In this range of the parameters $\{e, l\}$, we find that the mix component $\{g_{el}\}$ lies in the range of $\{-16, 0\}$. In this case, we see that the range of the growth of the amplitude of $\{g_{uu}\}$ remains in the regime of $\{-8, +8\}$ for the parameters $\{e, l\}$. Explicitly, this signifies that the five dimensional topological Einstein–Yang–Mills black holes are thermodynamically unstable in the limit of a large e and a positive l . Thus, the order higher entropy corrections are required for a large e in order to stabilize the five dimensional topological Einstein–Yang–Mills black hole system, which can easily be extracted from positivity of the components of the state-space metric tensor. Similarly, Figure 3 shows the nature of $\{g_{el}\}$ component of the state-space metric tensor. We find that the mix component

$\{g_{el}\}$ takes an uniform decreasing value from zero to -16 in both the limit of the parameter l and for the increasing value of e . In this limit of $\{e, l\}$, the local fluctuation of the entropy of the five dimensional topological Einstein–Yang–Mills black hole as depicted in Figures 1–3 illustrates the state-space stability properties of the five dimensional topological Einstein–Yang–Mills black hole ensemble. In short, the self pair fluctuations involving $\{e, l\}$, as defined by the metric tensor $\{g_{ij} \mid i, j = e, l\}$, have both positive and negative numerical values, and thus the five dimensional topological Einstein–Yang–Mills black hole are stable only in a particular domain of the vacuum parameters.

Figure 1. The ee component of Ruppeiner metric tensor plotted as the function of $\{e, l\}$, describing the fluctuations in five dimensional topological Einstein–Yang–Mills black hole configurations.

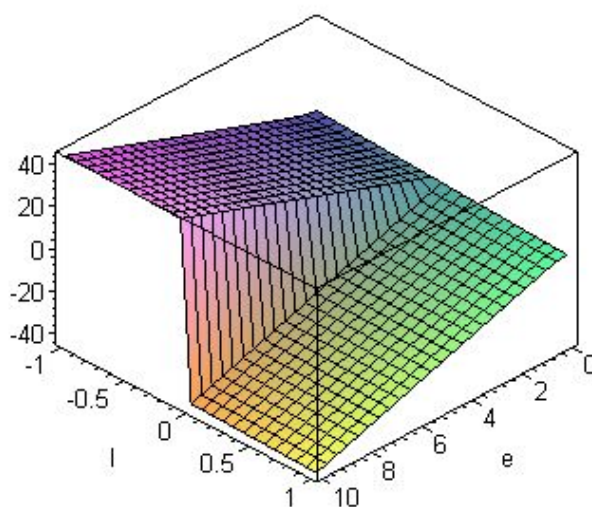


Figure 2. The ll component of Ruppeiner metric tensor plotted as the function of $\{e, l\}$, describing the fluctuations in five dimensional topological Einstein–Yang–Mills black hole configurations.

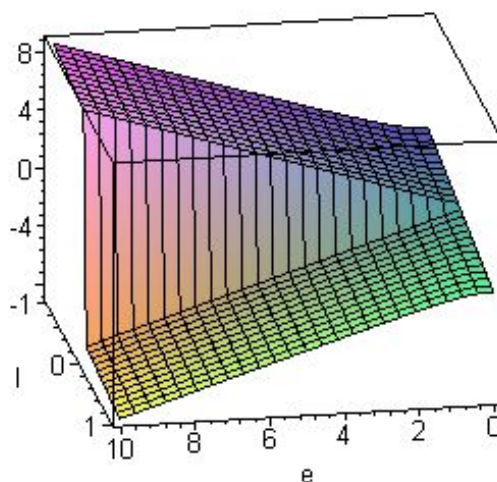
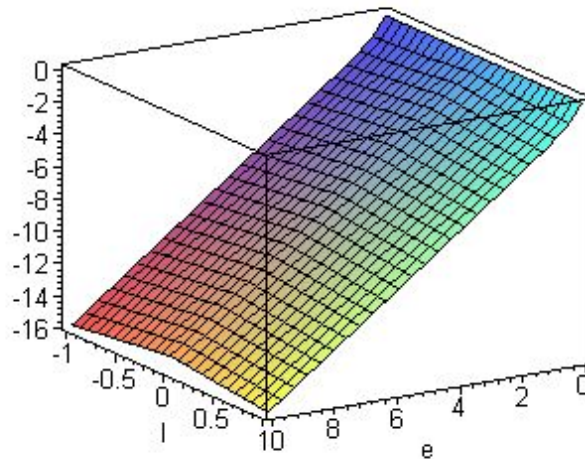


Figure 3. The el component of Ruppeiner metric tensor plotted as the function of $\{e, l\}$, describing the fluctuations in five dimensional topological Einstein–Yang–Mills black hole configurations.



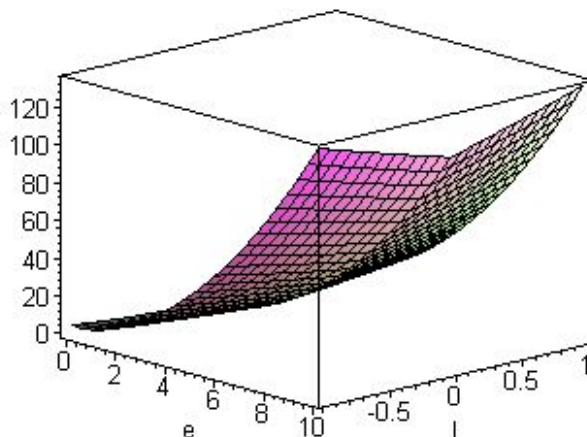
From the above expression of the metric tensor, it is not difficult to see that the determinant of the metric tensor can be expressed in the following form

$$g = \frac{9}{16} V_3^2 \frac{(1+f)^2}{f^3 (l^2 + 8e^2)} \left((16f + 38)e^4 + (10f + 14)l^2 e^2 + (f + 1)l^4 \right) \tag{12}$$

where the factor f is defined as per the Equation (10). Here with, we see that the five dimensional topological Einstein–Yang–Mills black holes remain stable under the effect of underlying thermodynamical fluctuation of $\{e, l\}$ in a chosen domain.

In this case, the ensemble stability of the five dimensional topological Einstein–Yang–Mills black holes can be determined in terms of the values of the regulation parameters e, l . This follows from the behavior of the determinant of metric tensor. Notice that the determinant of the metric tensor tends to a well-defined positive value when the vacuum parameters take relatively larger absolute values, viz. $e \rightarrow 10$ and $l \rightarrow \pm 1$. For $e \in (0, 10)$ and $l \in (-1, 1)$, Figure 4 shows that the determinant of the metric tensor lies in the interval $(0, 140)$. In fact, we find that the positivity of g increases as the values of (e, l) are increased from origin to $(10, \pm 1)$. In such cases, we find that the surface defined by the fluctuations of $\{e, l\}$ is stable. When only one of the parameter is allowed to vary, the stability of the underlying black hole configuration is determined by the positivity of the first principle minor. In other words, this amounts to the positivity statement of the ee component of the Ruppeiner metric tensor. The above graphical properties and positivity of the state-space quantities provide the underlying stability properties of the two parameter topological Einstein–Yang–Mills black holes in five space-time dimensions.

Figure 4. The determinant of Ruppeiner metric tensor plotted as the function of $\{e, l\}$, describing the fluctuations in five dimensional topological Einstein–Yang–Mills black hole configurations.



To examine the metric structure properties of the above fluctuations, we may compute the fluctuations of the metric tensor g_{ij} . For a given intrinsic surface of $\{e, l\}$, these fluctuations are precisely given by the following Christoffel symbols

$$\begin{aligned}
 \Gamma_{eee} &= -24 V_3 \frac{(16 e^2 + 5 l^2) e^3}{f (l^2 + 8 e^2)^2 l} & (13) \\
 \Gamma_{eel} &= -\frac{3}{4} V_3 \frac{(64 f e^4 + 20 l^2 e^2 + 16 l^2 f e^2 + l^4 f + l^4)}{f (l^2 + 8 e^2)^2} \\
 \Gamma_{ele} &= -\frac{3}{4} V_3 \frac{(64 f e^4 + 20 l^2 e^2 + 16 l^2 f e^2 + l^4 f + l^4)}{f (l^2 + 8 e^2)^2} \\
 \Gamma_{ell} &= -72 V_3 \frac{e^5}{f (l^2 + 8 e^2)^2 l} \\
 \Gamma_{lle} &= -72 V_3 \frac{e^5}{f (l^2 + 8 e^2)^2 l} \\
 \Gamma_{lll} &= -\frac{3}{8} V_3 \frac{(120 e^4 + 64 f e^4 + 20 l^2 e^2 + 16 l^2 f e^2 + l^4 f + l^4)}{f (l^2 + 8 e^2)^2}
 \end{aligned}$$

In this case, we find that the underlying thermodynamic configuration has no global fluctuation and the associated correlation length vanishes identically with the following Ruppeiner scalar curvature

$$R(e, l) = 0, \forall (e, l) \in \mathcal{M}_2 \tag{14}$$

The global stability properties of the two parameter topological Einstein–Yang–Mills black holes in five space-time dimensions follow from the underlying state-space scalar curvature. As, in this case, we find that the scalar curvature vanishes identically for all values of the black hole parameters. This shows that the fluctuating five dimensional topological Einstein–Yang–Mills black holes correspond to a noninteracting statistical configuration. In short, the above observations of the state-space geometry indicates that although the five dimensional topological Einstein–Yang–Mills black holes are non-interacting in the global sense, they correspond to a stable statistical configuration in a specific

domain of the vacuum parameters. Namely, when the parameter $\{e, l\}$ are allowed to fluctuate, we see that there exists certain domain of the vacuum parameters in which some of the component can fail to remain positive, thus incurring a local statistical instability. This observation follows from the fact that there are non-trivial instabilities at the local level of the vacuum fluctuations. From the above observation, it can be seen that the iterative procedure of vacuum parameters can be replaced by a statistically directed method of the state-space geometry. This formulation incorporates fluctuation of the parameters which follows the non-linearity Gaussian approximation about an equilibrium topological Einstein–Yang–Mills black hole system.

Without loss of the generality, for the pictorial representation of the thermodynamic quantities, we may as well choose the phase space volume to be unity, viz. $V_3 := 1$.

3.2. Higher Dimensional Black Holes

In this subsection, we illustrate the role of state-space geometry to the arbitrary higher dimensional topological Einstein–Yang–Mills black holes. In the highly growing space-time dimension, the entropy maximization is necessary in order to define the statistically stable limit of the field theory vacuum. Notice that, for the entropy maximization procedure, the Ruppeiner geometric state-space constraints as defined in the Section 2 are governed by the entropy flow equations. From the [42], the entropy of a topological Einstein–Yang–Mills black hole in any space-time dimension $D = 1 + n$ can be expressed as

$$S(l, e) := \frac{1}{8} V \sqrt{2} \sqrt{\frac{n-2}{n}} l \left(1 + \sqrt{1 + \frac{4ne^2}{(n-2)l^2}}\right)^{(n-1)} \tag{15}$$

To simplify the subsequent expression, we define a level function f_n as

$$f_n := (l^2 + 4e^2)n - 2l^2 \tag{16}$$

Thence, from the definition of Hessian of the entropy Equation (15), we find the following expressions for the components of the metric tensor

$$\begin{aligned} g_{ll} &= -\frac{1}{2}\sqrt{2} \left(4ne^2 \sqrt{\frac{f_n}{(n-2)l^2}} + l^2 + l^2 \sqrt{\frac{f_n}{(n-2)l^2}}\right) V \sqrt{\frac{n-2}{n}} \\ &\quad \left(1 + \sqrt{\frac{f_n}{(n-2)l^2}}\right)^{(n-3)} (n-1) ne^2 \left/ \left(\sqrt{\frac{f_n}{(n-2)l^2}} l^3 f_n\right)\right. \\ g_{el} &= \frac{1}{2}\sqrt{2} \left(4ne^2 \sqrt{\frac{f_n}{(n-2)l^2}} + l^2 + l^2 \sqrt{\frac{f_n}{(n-2)l^2}}\right) V \sqrt{\frac{n-2}{n}} \\ &\quad \left(1 + \sqrt{\frac{f_n}{(n-2)l^2}}\right)^{(n-3)} (n-1) ne \left/ \left(l^2 f_n \sqrt{\frac{f_n}{(n-2)l^2}}\right)\right. \\ g_{ee} &= -\frac{1}{2}\sqrt{2} \left(4ne^2 \sqrt{\frac{f_n}{(n-2)l^2}} + l^2 + l^2 \sqrt{\frac{f_n}{(n-2)l^2}}\right) V \sqrt{\frac{n-2}{n}} \\ &\quad \left(1 + \sqrt{\frac{f_n}{(n-2)l^2}}\right)^{(n-3)} (n-1) n \left/ \left(\sqrt{\frac{f_n}{(n-2)l^2}} f_n l\right)\right. \end{aligned} \tag{17}$$

Notice that the local stability characteristic of the higher dimensional topological Einstein–Yang–Mills black holes follows from the positivity of the heat capacities $\{g_{ee}, g_{ll}\}$ of the state-space metric tensor. These are basically the diagonal components of the metric tensor associated with entropy maximization of a chosen ensemble of the higher dimensional topological Einstein–Yang–Mills black holes. For the choice of $V = 1$, the explicit graphical view of the above mentioned local fluctuations is depicted in Figures 5 and 6. In the regime of $e, l \in (0, 1)$, we see that the amplitude of $\{g_{ee}\}$ takes a value of the order $-8 \times 10^{+07}$. In this range of the parameters $\{e, l\}$, we find that the component $\{g_{ll}\}$ lies in the range of $(-5 \times 10^{+10}, 0)$. In this case, we observe that the growth of the amplitude of $\{g_{ee}, g_{ll}\}$ happens in the same distinct limit of $\{e, l\}$, that is a large e and a small l . In the above regime, for a given value of e up to 0.15, the system is nearly stable up to in the range of $l \in (0.2, 1)$. Smaller values of the l tend the system towards an instability. The entropy of a large e and a small l leads to an intrinsic state-space instability and thus can be the cause the black hole to disappear. This is also forbidden by the black hole remnant hypothesis. As shown in the Equation (17), the entropy flow, namely the heat capacities, depends on the black hole parameters, and thus changing the value of a parameter or the fluctuation in $\{e, l\}$ can affect the stability characteristics of the chosen higher dimensional topological Einstein–Yang–Mills black hole ensemble. Thus, the diagonal component of the state-space metric tensor should be positive for which the fluctuations provide a set of values of $\{e, l\}$ from which one can determine the required local values of the flow parameters e and l . This signifies that the entropy extremization could characterize the underlying thermodynamic instability of an ensemble of chosen black holes. Here, one is only required to chose a specific domain of the parameters $\{e, l\}$ such that the desired system remain in a well balanced limit of the entropy flow parameters. Further, we notice from Figure 7 that the mix component $\{g_{el}\}$ of the state-space metric tensor has a positive value under the entropy fluctuation. Interestingly, we find that all the local fluctuations happen in a small limit of the flow parameter l , and a large limit of the flow parameter e , where higher value of e happen to cause an instability. Figure 7 shows that the higher dimensional topological Einstein–Yang–Mills black holes cannot flow throughout the vacuum, as long as there is a positive local heat capacity. In this examination, the other parameters have to be kept constant in order to determine the limiting parametric stability of the higher dimensional topological Einstein–Yang–Mills black hole ensemble. In this sense, we see that Figures 5–7 illustrate the local fluctuation properties of ensemble of arbitrary dimensional topological Einstein–Yang–Mills black holes under the entropic flow of the $\{e, l\}$. In fact, both the self pair fluctuations involving $\{e, l\}$, as defined by the metric tensor $\{g_{ij} \mid i, j = e, l\}$ have only the negative numerical values, while the mix component $\{g_{el}\}$ does not. More precisely, in order to see the global stability limit, we require that the determinant of the metric tensor should be also positive in a chosen domain of the parameters $\{e, l\}$. Thus, for the values from a given set of fluctuating $\{e, l\}$ as shown in Figures 5–7, the illustration of the above type of ensemble of higher dimensional topological Einstein–Yang–Mills black holes happens to be true locally. This is because of the fact that the determinant of the state-space metric tensor vanishes identically for all values of $\{e, l\}$. Thus, the entropy extremization of higher dimensional topological Einstein–Yang–Mills black hole ensemble for given $\{e, l\}$, in order to find a positive determinant regime, would require further higher derivative stringy corrections or quantum loop corrections to the entropy in order to keep an ensemble of topological Einstein–Yang–Mills black holes globally stable.

Figure 5. The ee component of Ruppeiner metric tensor plotted as the function of $\{e, l\}$, describing the fluctuations in six dimensional topological Einstein–Yang–Mills black hole configurations.

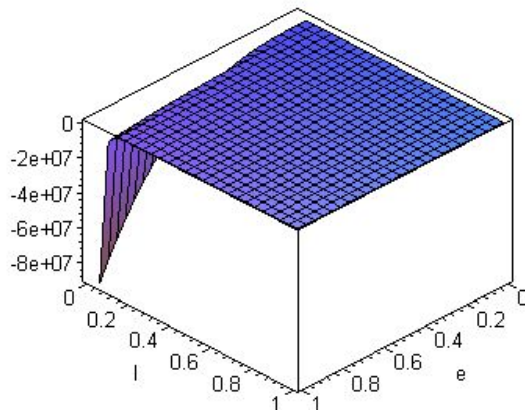


Figure 6. The ll component of Ruppeiner metric tensor plotted as the function of $\{e, l\}$, describing the fluctuations in six dimensional topological Einstein–Yang–Mills black hole configurations.

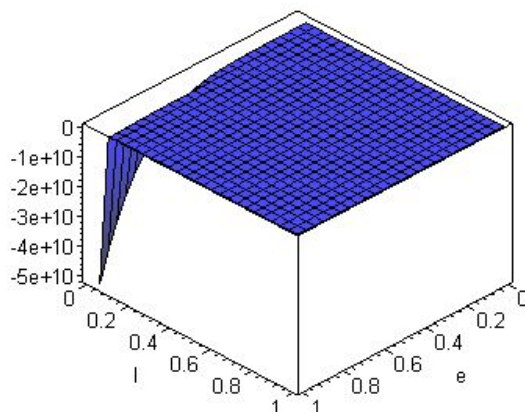
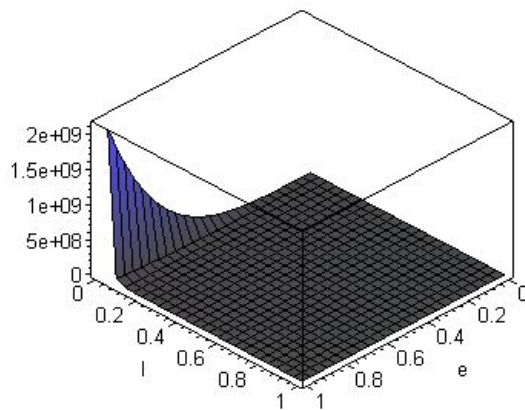


Figure 7. The el component of Ruppeiner metric tensor plotted as the function of $\{e, l\}$, describing the fluctuations in six dimensional topological Einstein–Yang–Mills black hole configurations.



In this case, since the determinant of the state-space metric tensor vanishes identically for all values of the parameters $\{e, l\}$, there is no question of computing the state-space scalar curvature. From the perspective of intrinsic geometry, we find that the Christoffel symbols of arbitrary topological Einstein–Yang–Mills black hole can be expressed as the following expressions

$$\begin{aligned}
 \Gamma_{eee} &= -\frac{(n-1)V\sqrt{2}\sqrt{\frac{n-2}{n}}\left(1+\sqrt{\frac{f_n}{(n-2)l^2}}\right)^{(n-4)}n^2e}{\left(\sqrt{\frac{f_n}{(n-2)l^2}}l^3f_n^2(n-2)\right)}\left(\Gamma_{eee}^{(1)}+\sqrt{\frac{f_n}{(n-2)l^2}}\Gamma_{eee}^{(2)}\right) \\
 \Gamma_{eel} &= \frac{1}{\sqrt{2}}\frac{V\sqrt{\frac{n-2}{n}}\left(1+\sqrt{\frac{f_n}{(n-2)l^2}}\right)^{(n-4)}(n-1)n}{\left(\sqrt{\frac{f_n}{(n-2)l^2}}l^4f_n^2(n-2)\right)}\left(\Gamma_{eel}^{(1)}+\sqrt{\frac{f_n}{(n-2)l^2}}\Gamma_{eel}^{(2)}\right) \\
 \Gamma_{ele} &= \frac{1}{2}\frac{V\sqrt{2}\sqrt{\frac{n-2}{n}}\left(1+\sqrt{\frac{f_n}{(n-2)l^2}}\right)^{(n-4)}(n-1)n}{\left(\sqrt{\frac{f_n}{(n-2)l^2}}l^4f_n^2(n-2)\right)}\left(\Gamma_{ele}^{(1)}+\sqrt{\frac{f_n}{(n-2)l^2}}\Gamma_{ele}^{(2)}\right) \\
 \Gamma_{ell} &= -\frac{(n-1)V\sqrt{2}\sqrt{\frac{n-2}{n}}\left(1+\sqrt{\frac{f_n}{(n-2)l^2}}\right)^{(n-4)}ne}{\left(\sqrt{\frac{f_n}{(n-2)l^2}}l^5f_n^2(n-2)\right)}\left(\Gamma_{ell}^{(1)}+\sqrt{\frac{f_n}{(n-2)l^2}}\Gamma_{ell}^{(2)}\right) \\
 \Gamma_{lle} &= -\frac{(n-1)V\sqrt{2}\sqrt{\frac{n-2}{n}}\left(1+\sqrt{\frac{f_n}{(n-2)l^2}}\right)^{(n-4)}ne}{\left(\sqrt{\frac{f_n}{(n-2)l^2}}l^5f_n^2(n-2)\right)}\left(\Gamma_{lle}^{(1)}+\sqrt{\frac{f_n}{(n-2)l^2}}\Gamma_{lle}^{(2)}\right) \\
 \Gamma_{lll} &= \frac{1}{2}\frac{V\sqrt{2}\sqrt{\frac{n-2}{n}}\left(1+\sqrt{\frac{f_n}{(n-2)l^2}}\right)^{(n-4)}(n-1)ne^2}{\left(\sqrt{\frac{f_n}{(n-2)l^2}}l^6f_n^2(n-2)\right)}\left(\Gamma_{lll}^{(1)}+\sqrt{\frac{f_n}{(n-2)l^2}}\Gamma_{lll}^{(2)}\right) \quad (18)
 \end{aligned}$$

where the factors $\{\Gamma_{ijk}^{(1)}, \Gamma_{ijk}^{(2)}|i, j, k \in \{e, l\}\}$ of arbitrary Ruppeiner metric tensor are relegated to Appendix A.

4. Weinhold Geometry

In this section, we illustrate the role of thermodynamic geometry from the perspective of the energy minimization, that is here the minimization of the ADM mass of the topological Einstein–Yang–Mills black hole in space-time dimension $D = 5$. Given an ensemble of such black hole configurations, the optimization of the energy is necessary in order to define the vacuum stability of the Yang–Mills gauge theory with a non-trivial topological black hole, where not only the field theory is considered to have a fluctuating vacuum but also an imminent black hole in the space-time background of the Yang–Mills vacuum ensemble. To illustrate the hypothesis, we shall first consider the case of five dimensional theory and then in the next subsection generalize it to an ensemble of arbitrary dimensional topological Einstein–Yang–Mills black holes. It is worth mentioning that the energy minimization is intrinsically

same to the entropy maximization up to a Legendre transformation. Thus, we may notice that the flow equations and the analysis of the parametric stability constraint in the sense of the Weinhold geometry follows directly up to a sign with the definition of the Ruppeiner geometry. Both of these thermodynamic geometries are intertwined to each other, as we have defined then in the Section 2.

4.1. Five Dimensional Black Holes

From the [42], the ADM mass of a topological Einstein–Yang–Mills black hole in space-time dimension $D = 5$ is given by

$$M(e, l) := -\frac{1}{3} e^2 \left(\ln\left(\frac{1}{4} l^2 + \frac{1}{4} l (l^2 + 8 e^2)\right) - \frac{1}{2} \right) - \frac{1}{24} l^2 - \frac{1}{24} l (l^2 + 8 e^2) \tag{19}$$

With the notions of the thermodynamic geometry, the Legendre associated Weinhold line element can be expressed as

$$ds^2 = \left(\frac{\partial^2}{\partial e^2} M(e, l) \right) de^2 + 2 \left(\frac{\partial^2}{\partial l \partial e} M(e, l) \right) de dl + \left(\frac{\partial^2}{\partial l^2} M(e, l) \right) dl^2 \tag{20}$$

To simplify the expression of the determinant of the metric tensor, the appropriate scaling function turns out to be

$$b := l + l^2 + 8 e^2 \tag{21}$$

For the above given mass, the computation of the Hessian matrix shows the following expressions for the components of the Weinhold metric tensor

$$\begin{aligned} g_{ee} &= \frac{1}{3b^2} (-320 e^4 - 64 l e^2 - 96 l^2 e^2 - 32 l^3 e^2 - 128 l e^4 - 3 l^4 \\ &\quad + 64 \ln(2) l e^2 + 4 \ln(2) l^2 + 8 \ln(2) l^3 + 4 \ln(2) l^4 + 256 \ln(2) e^4 \\ &\quad + 64 \ln(2) l^2 e^2 - 2 \ln(lb) l^4 - 128 \ln(lb) e^4 - 32 \ln(lb) l e^2 \\ &\quad - 2 l^5 - 2 \ln(lb) l^2 - 4 \ln(lb) l^3 - 32 \ln(lb) l^2 e^2 + l^2) \\ g_{el} &= -\frac{2e}{3b^2 l} (2 l^2 + 6 l^3 + 16 l e^2 + 5 l^4 + 32 l^2 e^2 + 64 e^4 \\ &\quad + l^5 + 16 l^3 e^2 + 64 l e^4) \\ g_{ll} &= \frac{1}{12b^2 l^2} (8 l^2 e^2 + 64 l e^4 - 52 l^4 e^2 - 64 e^4 l^2 + 256 e^6 \\ &\quad - l^4 - 5 l^5 - 7 l^6 - 3 l^7 - 48 l^5 e^2 - 192 l^3 e^4) \end{aligned} \tag{22}$$

In this case, we see that the heat capacities have rather diverse characters. For the case of $V = 1$, the heat capacities $\{g_{ee}, g_{ll}\}$ are shown in Figures 8 and 9. Here, in the interval of $e, l \in (0, 1)$, the amplitude of $\{g_{ll}\}$ takes a positive value of the order 200. In this range of the parameters $\{e, l\}$, Figure 8 shows that the component $\{g_{ee}\}$ lies in the range of $(-4, +6)$. In this case, we hereby observe that the fluctuations of both the $\{g_{ee}, g_{ll}\}$ do not occur with a positive amplitude of the fluctuations. Namely, the ee component fluctuations are generically present near the origin of the flow parameters, while this is not the case for the ll component. We see that the ll component energy fluctuations are largely present for a large e and a small l . Figure 10 shows that the corresponding mix component of the complex ADM

mass flow fluctuation, in which the el component of the Weinhold metric takes a maximum amplitude of the order -16 . The above plots may change for a different vacuum black hole and for a different field theory, as well. The values of e and l are sensitive to higher derivative and higher order corrections as well. This analysis can further be extended for a different Lagrangian of the theory and the background space-time black hole ensemble.

Figure 8. The ee component of Weinhold metric tensor plotted as the function of $\{e, l\}$, describing the fluctuations in five dimensional topological Einstein–Yang–Mills black hole configurations.

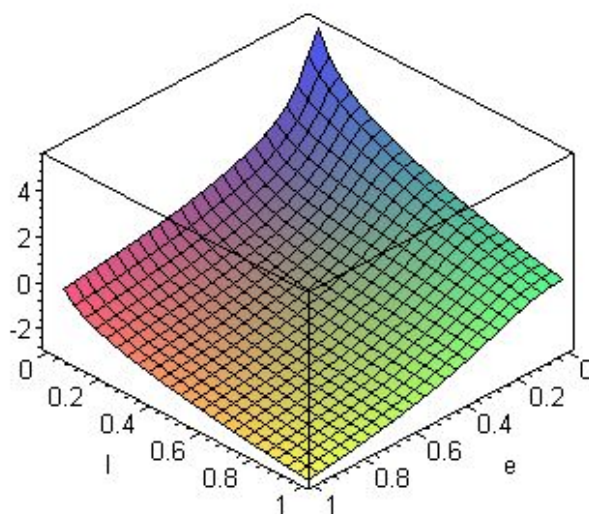


Figure 9. The ll component of Weinhold metric tensor plotted as the function of $\{e, l\}$, describing the fluctuations in five dimensional topological Einstein–Yang–Mills black hole configurations.

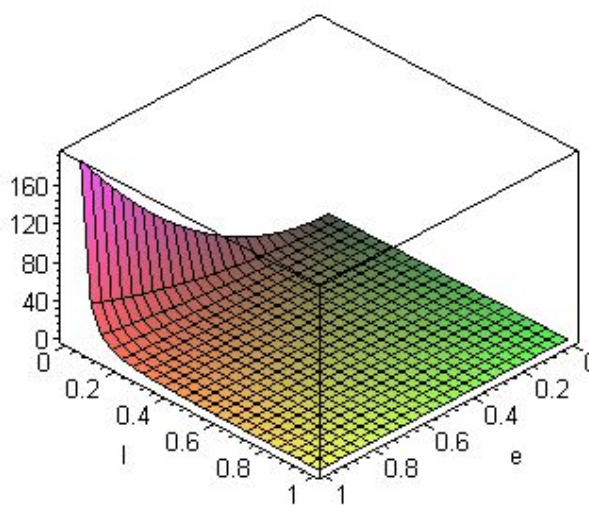
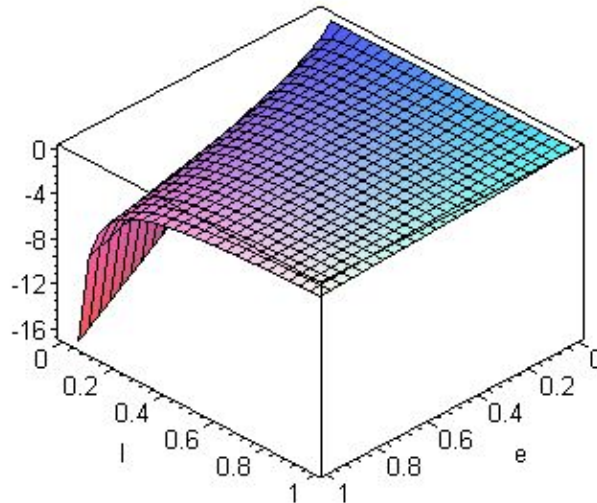


Figure 10. The el component of Weinhold metric tensor plotted as the function of $\{e, l\}$, describing the fluctuations in five dimensional topological Einstein–Yang–Mills black hole configurations.



To illustrate the metric structure properties of the above mass fluctuations, we now offer the fluctuation properties of the metric tensor g_{ij} . For a given intrinsic Weinhold surface of $\{e, l\}$, these fluctuations are precisely depicted by the following Christoffel symbols

$$\begin{aligned}
 \Gamma_{eee} &= -\frac{32}{3b^3} (e (3l^2 + 6l^3 + 12le^2 + 3l^4 + 12l^2e^2 + 32e^4)) \\
 \Gamma_{eel} &= -\frac{1}{3lb^3} (2l^3 + 8l^4 + 11l^5 + 192le^4 + 512le^6 + 24l^5e^2 \\
 &\quad + 192l^3e^4 + l^7 + 6l^6 + 512e^6 + 24l^4e^2 + 384e^4l^2) \\
 \Gamma_{ele} &= -\frac{1}{3lb^3} (2l^3 + 8l^4 + 11l^5 + 192le^4 + 512le^6 + 24l^5e^2 \\
 &\quad + 192l^3e^4 + l^7 + 6l^6 + 512e^6 + 24l^4e^2 + 384e^4l^2) \\
 \Gamma_{ell} &= \frac{1}{3l^2b^3} (e (2l^3 + 6l^4 + 16l^2e^2 + 7l^5 + 192le^4 + 3l^6 \\
 &\quad + 512e^6 - 24l^4e^2 + 192e^4l^2)) \\
 \Gamma_{lle} &= \frac{1}{3l^2b^3} (e (2l^3 + 6l^4 + 16l^2e^2 + 7l^5 + 192le^4 + 3l^6 \\
 &\quad + 512e^6 - 24l^4e^2 + 192e^4l^2)) \\
 \Gamma_{lll} &= -\frac{1}{24l^3b^3} (1536le^6 + 120l^5e^2 + 192l^3e^4 + 9l^7 + 3l^6 \\
 &\quad + 48l^4e^2 + 16l^3e^2 + 192e^4l^2 + 168l^6e^2 + 384l^4e^4 \\
 &\quad + 9l^8 + 3l^9 + 72l^7e^2 + 576l^5e^4 + 1536l^3e^6 + 4096e^8 \\
 &\quad + 1536l^2e^6)
 \end{aligned} \tag{23}$$

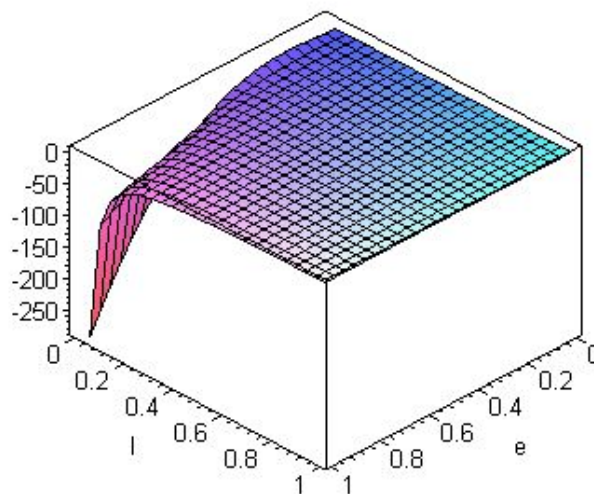
Here the determinant of the metric tensor reduces to the following formula

$$g = \frac{1}{36l^2b^3} \sum_{i=0}^4 r_i(l)e^{2i} \tag{24}$$

where the coefficients $r_i(l)$ are given in Appendix B.

As mentioned in the previous section for the fluctuating entropy of an ensemble of five dimensional topological Einstein–Yang–Mills black hole, we see in this case that the ensemble stability of the fluctuating configuration can be determined in terms of the values of the determinant of the Weinhold metric tensor, as the function of the mass flow parameter $\{e, l\}$, as defined above. Furthermore, the global behavior of the system follows from the determinant of fluctuation metric tensor. For the cases of $V = \pm 1$, we observe that the determinant of the Weinhold metric tensor tends to a negative value. Namely, we see from Figure 11 that the peak of the determinant of the Weinhold metric tensor is of the order -300 . As in the case of the local energy fluctuations of the five dimensional topological Einstein–Yang–Mills black holes, we find that the global energy fluctuations also happen for a small value of the parameter l and a large value of the charge e . When only one of the parameter is allowed to vary, the stability of the five dimensional topological Einstein–Yang–Mills black hole ensemble is determined by the positivity of the first principle minor $p_1 := g_{ee}$. Physically, the above qualitative demonstrations of the energy fluctuations illustrate the parametric stability properties of an ensemble of two parameter five dimensional topological Einstein–Yang–Mills black holes.

Figure 11. The determinant of Weinhold metric tensor plotted as the function of $\{e, l\}$, describing the fluctuations in five dimensional topological Einstein–Yang–Mills black hole configurations.



With convention $\tilde{b} := \ln(l(l + l^2 + 8e^2))$, we find that the scalar curvature possesses the following non-trivial expression

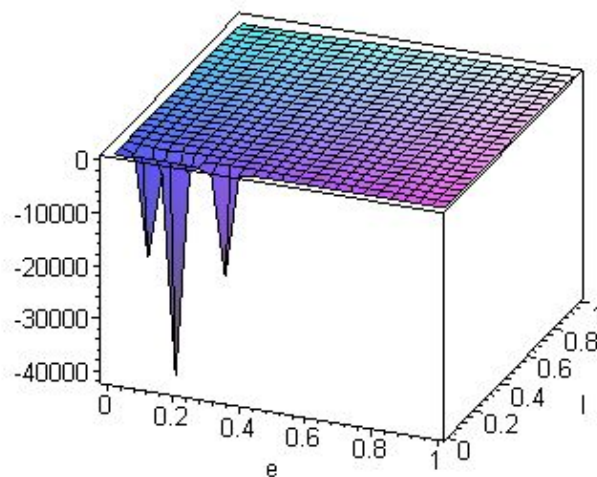
$$R = 12 \frac{\sum_{i=0}^7 R_i(l)e^{2i}}{(\sum_{i=0}^4 r_i(l)e^{2i})^2} \tag{25}$$

where the factors in the numerator are given in Appendix B. It is worth mentioning that the coefficients $\{r_i(l) | i = 0, 1, 2, 3, 4\}$, appearing in the denominator of the scalar curvature, remain the functions as those given in Appendix B for the numerator of the determinant of the metric tensor.

In general, it is worth mentioning that the long range correlations are characterized as per the definition of the scalar curvature. Namely, the global stability properties of the five dimensional topological Einstein–Yang–Mills black hole ensemble follow from the corresponding thermodynamic

scalar curvature. In particular, for the range of $e, l \in (0, 1)$, Figure 12 shows that the scalar curvature has a negative amplitude of order -40000 . This shows that the underlying five dimensional topological Einstein–Yang–Mills black hole configuration is an interacting system. The negative sign of the scalar curvature signifies the attractive nature of the statistical interactions. For the case of $e \in (0, 1)$ and $l \in (0, 1)$, we notice from Figure 12 that there exist a number of large negative peak of the global interactions of the order -20000 to -40000 . In this sense, up to a small range of e and l , the two parameter five dimensional topological Einstein–Yang–Mills black holes behave as a stable configuration, however an increasing value of $\{e, l\}$ cannot increase the limit of the parametric stability, as it could make a negative value of the determinant of the metric tensor. Thus, Figure 12 indicates the interaction properties of the underlying five dimensional topological Einstein–Yang–Mills black hole configuration when the parameters $\{e, l\}$ are allowed to fluctuate. The above instability analysis shows the above black hole system for small values of the vacuum parameters is highly sensitivity to the statistical fluctuations.

Figure 12. The Weinhold curvature scalar plotted as the function of $\{e, l\}$, describing the fluctuations in five dimensional topological Einstein–Yang–Mills black hole configurations.



4.2. Higher Dimensional Black Holes

From the [42], the ADM mass of a topological Einstein–Yang–Mills black hole in arbitrary space-time dimension $D = 1 + n$ can be expressed by

$$M(e, l) := -\frac{2}{n-1} \left(\sqrt{\frac{n-2}{2n}} l \sqrt{1 + \sqrt{1 + \frac{4ne^2}{(n-2)l^2}}} \right)^{(n-4)} \times \left(\frac{1}{4} \frac{(n-2)l^2 \left(1 + \sqrt{1 + \frac{4ne^2}{(n-2)l^2}}\right)^2}{n^2} + \frac{e^2}{n-4} \right) \tag{26}$$

In this case, let the scaling function be defined as

$$b_n := \frac{l^2 n - 2l^2 + 4n e^2}{(n - 2) l^2} \tag{27}$$

Thence, for a given mass of the five dimensional extremal topological Einstein–Yang–Mills black hole, we find the following components of Weinhold metric tensor

$$\begin{aligned} g_{ee} &= -16(e^2 n^2 + e^2 \sqrt{b_n} n^2 - 2e^2 \sqrt{b_n} n + l^2 \sqrt{b_n} n + l^2 n - 2l^2 - 2l^2 \sqrt{b_n}) 2^{(-1/2n)} \\ &\quad \left(\sqrt{\frac{n-2}{n}} l \sqrt{1 + \sqrt{b_n}}^n n^2 / ((n-2)^2 l^6 (1 + \sqrt{b_n})^4 (n-1)(n-4) \sqrt{b_n}) \right) \\ g_{el} &= -64e(5n^2 e^4 + e^4 n^2 \sqrt{b_n} + 3e^2 l^2 \sqrt{b_n} n^2 + 5n^2 e^2 l^2 - 6e^2 l^2 \sqrt{b_n} n \\ &\quad - 10n e^2 l^2 + l^4 \sqrt{b_n} n^2 + l^4 n^2 - 4l^4 n - 4l^4 \sqrt{b_n} n + 4l^4 \sqrt{b_n} + 4l^4) \\ &\quad 2^{(-1/2n)} \left(\sqrt{\frac{n-2}{n}} l \sqrt{1 + \sqrt{b_n}}^n n^2 / ((n-2)^3 l^9 (1 + \sqrt{b_n})^6 \sqrt{b_n} (n-1)) \right) \\ g_{ul} &= -32(30l^6 \sqrt{b_n} n^2 - 9l^6 \sqrt{b_n} n^3 + l^6 \sqrt{b_n} n^4 - 44l^6 \sqrt{b_n} n + 108n^2 e^2 l^4 \\ &\quad - 45n^3 e^2 l^4 + 6n^4 e^2 l^4 + 78n^2 e^4 l^2 - 57n^3 e^4 l^2 + 9n^4 e^4 l^2 - 84n e^2 l^4 \\ &\quad + 2n^4 e^6 + 24l^6 + l^6 n^4 - 12n^3 e^6 - 9l^6 n^3 + 30l^6 n^2 - 44l^6 n + 24l^6 \sqrt{b_n} \\ &\quad + 4n^4 e^2 l^4 \sqrt{b_n} + 76n^2 e^2 l^4 \sqrt{b_n} - 31n^3 e^2 l^4 \sqrt{b_n} - 21n^3 e^4 l^2 \sqrt{b_n} \\ &\quad + 30n^2 e^4 l^2 \sqrt{b_n} - 60n e^2 l^4 \sqrt{b_n} + 3\sqrt{b_n} n^4 e^4 l^2) 2^{(-1/2n)} \\ &\quad \left(\sqrt{\frac{n-2}{n}} l \sqrt{1 + \sqrt{b_n}}^n / ((n-2)^3 l^{10} (1 + \sqrt{b_n})^5 (n-1) \sqrt{b_n}) \right) \end{aligned} \tag{28}$$

As mentioned the previous case, we find in this case, in the range of $e \in (0, 1)$ and $l \in (-1, 1)$, that the fluctuation of the components $\{g_{ee}, g_{ul}\}$ lie in a negative interval. Namely, the components g_{ee} lie in $(-1.6, 0)$, while the components g_{ul} lie in $(-0.8, 0)$. This shows that the topological Einstein–Yang–Mills black hole in arbitrary space-time dimension $D = 1 + n$ are locally unstable configurations with respect to the fluctuations of the $\{e, l\}$. In fact, the range of the growth of $\{g_{ee}, g_{ul}\}$ happens to be in the same negative limit of the amplitude under the flow of the parameters $\{e, l\}$. Explicitly, from Figures 13 and 14 we observe that the of growth of the g_{aa} and g_{bb} takes place in the limit of a large l for all e . On the other hand, the component involving two distinct parameters of black hole has been depicted in Figure 15. In this case, we notice that Figure 15 shows that the el -component of the mass fluctuations lies in the interval $(-1.5, 1.5)$. Thus, for a given ensemble of higher dimensional topological Einstein–Yang–Mills black holes, the components of the metric tensor $\{g_{ij} \mid i, j = e, l\}$ indicate that the fluctuations involving the vacuum parameters $\{e, l\}$ have relatively meager positive numerical values and thus they are prone to yield a statistically unstable ensemble at this order of the ADM mass.

To discuss the thermodynamic properties of arbitrary topological Einstein–Yang–Mills black hole in $(1 + n)$ space-time dimensions, we introduce a new scaling function

$$c_n := l^2 n - 2l^2 + 4n e^2 = (n - 2) l^2 b_n \tag{29}$$

With this convention, we obtain the following Christoffel tensors

$$\begin{aligned}
 \Gamma_{eee} &= -\frac{162^{(-1/2n)} \left(\sqrt{\frac{n-2}{n}} l \sqrt{1 + \sqrt{\frac{c_n}{(n-2)l^2}}}\right)^n n^3 e}{((n-2)^2 l^8 \left(1 + \sqrt{\frac{c_n}{(n-2)l^2}}\right)^5 (n-1) \sqrt{\frac{c_n}{(n-2)l^2} c_n})} (\Gamma_{eee}^{(1)} + \sqrt{\frac{c_n}{(n-2)l^2}} \Gamma_{eee}^{(2)}) \\
 \Gamma_{eel} &= -\frac{1282^{(-1/2n)} \left(\sqrt{\frac{n-2}{n}} l \sqrt{1 + \sqrt{\frac{c_n}{(n-2)l^2}}}\right)^n n^2}{((n-2)^3 l^{11} \left(1 + \sqrt{\frac{c_n}{(n-2)l^2}}\right)^8 \sqrt{\frac{c_n}{(n-2)l^2} (n-1)c_n})} (\Gamma_{eel}^{(1)} + \sqrt{\frac{c_n}{(n-2)l^2}} \Gamma_{eel}^{(2)}) \\
 \Gamma_{ele} &= -\frac{1282^{(-1/2n)} \left(\sqrt{\frac{n-2}{n}} l \sqrt{1 + \sqrt{\frac{c_n}{(n-2)l^2}}}\right)^n n^2}{((n-2)^3 l^{11} \left(1 + \sqrt{\frac{c_n}{(n-2)l^2}}\right)^8 \sqrt{\frac{c_n}{(n-2)l^2} (n-1)c_n})} (\Gamma_{ele}^{(1)} + \sqrt{\frac{c_n}{(n-2)l^2}} \Gamma_{ele}^{(2)}) \\
 \Gamma_{ell} &= -\frac{64 \left(\sqrt{\frac{n-2}{n}} l \sqrt{1 + \sqrt{\frac{c_n}{(n-2)l^2}}}\right)^n e 2^{(-1/2n)} n^2}{((n-2)^4 l^{12} \left(1 + \sqrt{\frac{c_n}{(n-2)l^2}}\right)^7 (n-1) \sqrt{\frac{c_n}{(n-2)l^2} c_n})} (\Gamma_{ell}^{(1)} + \sqrt{\frac{c_n}{(n-2)l^2}} \Gamma_{ell}^{(2)}) \\
 \Gamma_{lle} &= -\frac{128 e 2^{(-1/2n)} \left(\sqrt{\frac{n-2}{n}} l \sqrt{1 + \sqrt{\frac{c_n}{(n-2)l^2}}}\right)^n n^2}{((n-2)^4 l^{12} \left(1 + \sqrt{\frac{c_n}{(n-2)l^2}}\right)^8 (n-1) \sqrt{\frac{c_n}{(n-2)l^2} c_n})} (\Gamma_{lle}^{(1)} + \sqrt{\frac{c_n}{(n-2)l^2}} \Gamma_{lle}^{(2)}) \\
 \Gamma_{lll} &= -\frac{64 \left(\sqrt{\frac{n-2}{n}} l \sqrt{1 + \sqrt{\frac{c_n}{(n-2)l^2}}}\right)^n}{((n-2)^4 l^{13} \left(1 + \sqrt{\frac{c_n}{(n-2)l^2}}\right)^7 \sqrt{\frac{c_n}{(n-2)l^2} c_n} (n-1))} (\Gamma_{lll}^{(1)} + \sqrt{\frac{c_n}{(n-2)l^2}} \Gamma_{lll}^{(2)})
 \end{aligned}
 \tag{30}$$

where the factors $\{\Gamma_{ijk}^{(1)}, \Gamma_{ijk}^{(2)} | i, j, k \in \{e, l\}\}$ are given in the Appendix C. In this case, we find the following determinant of the metric tensor

$$g = \frac{1}{2} \frac{\left(\left(\sqrt{\frac{n-2}{2n}} l \sqrt{1 + \sqrt{\frac{c_n}{(n-2)l^2}}}\right)^{(n-4)}\right)^2}{(l^{10} n^2 \left(1 + \sqrt{\frac{c_n}{(n-2)l^2}}\right)^8 c_n^5 (n-4) (n-1)^2 (n-2)^2)} \times (g_1 + g_2 \sqrt{\frac{c_n}{(n-2)l^2}}) \tag{31}$$

Interestingly, as the functions of $\{e, l\}$, it turns out after a simplification that both the factors $g_1(e, l)$ and $g_2(e, l)$ can be expressed as the following finite homogeneous polynomials

$$g_a := \sum_{i=1}^{10} g_{ai} e^{2i} l^{20-2i}, \quad a = 1, 2 \tag{32}$$

where both the coefficients $\{g_{1i}, g_{2i}\}$ can be defined as polynomials in dimension of the space $n \geq 6$. Explicitly, as the powers of the electric charge e , we find that the coefficients $\{g_{1i} \mid i = 1, \dots, 10\}$ give a particular degree 20 expression. In order to keep readability of the paper, we relegate the expression of the specific factors to the Appendix C. Similarly, as the powers of the electric charge e , it follows that the second series of factors $\{g_{2i} \mid i = 1, \dots, 9\}$ reduce to the degree 18 polynomials. Further, the explicit expression of the factors is provided in the Appendix C.

Figure 13. The ee component of the metric tensor plotted as the function of $\{e, l\}$, describing the fluctuations in six dimensional topological Einstein–Yang–Mills black hole configurations.

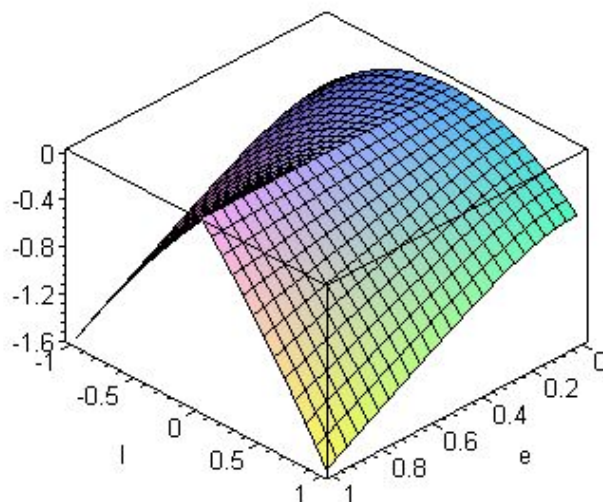


Figure 14. The ll component of the metric tensor plotted as the function of $\{e, l\}$, describing the fluctuations in six dimensional topological Einstein–Yang–Mills black hole configurations.

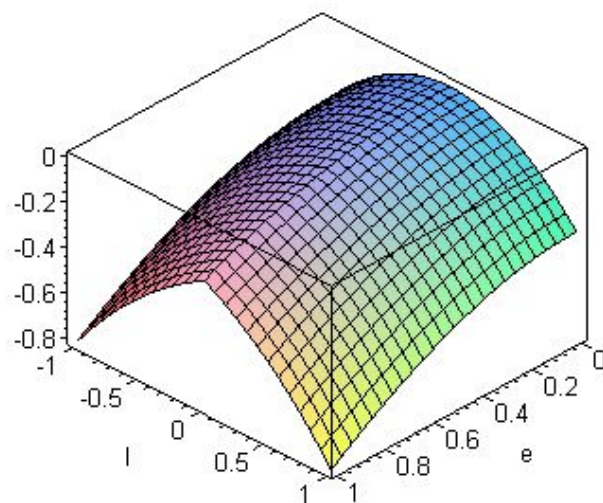
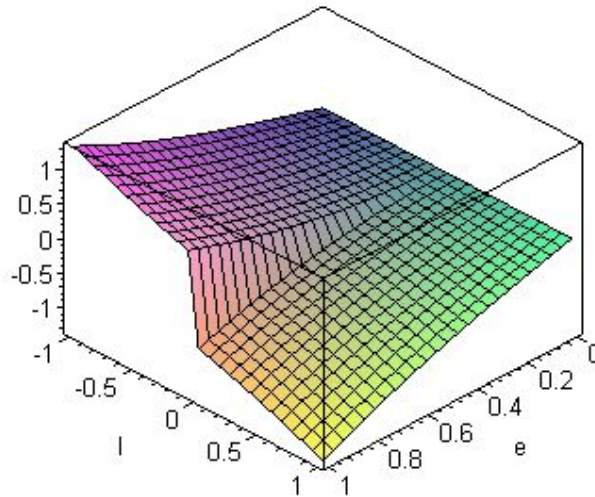


Figure 15. The el component of the metric tensor plotted as the function of $\{e, l\}$, describing the fluctuations in six dimensional topological Einstein–Yang–Mills black hole configurations.



As the function of $\{e, l\}$, the ensemble stability condition of the higher dimensional topological Einstein–Yang–Mills black holes follows from the positivity of the determinant of the metric tensor. In this case, we find that the determinant of the metric tensor generically tends to a negative value. For a typical value of $e \in (0, 1)$ and $l \in (-1, 1)$, Figure 16 shows that the determinant of the metric tensor lies in the interval $(-0.6, +0.2)$. Hereby, for a small e , we observe that the determinant of the metric tensor has an approximate value of $+0.15$. As we increase the value of the electric charge e , in the limit of a large $|l|$, the determinant of the metric tensor nearly takes a larger positive value of its amplitude. Thence, for a given l , in the limit of a large e , it increases sharply to a larger negative value of order -0.6 . When only one of the parameter is allowed to vary, the stability of the higher dimensional topological Einstein–Yang–Mills black hole configuration is determined by the positivity of the first principle minor $p_1 := g_{ee}$, see Figure 13. We further find that all the above mentioned qualitative picture remain valid for other values of n than the special case of $n = 5$. Thus, the above graphical descriptions of the principle minors offers a qualitative notion of the stability of the an ensemble of topological Einstein–Yang–Mills black holes in space-time dimensions $D \geq 5$.

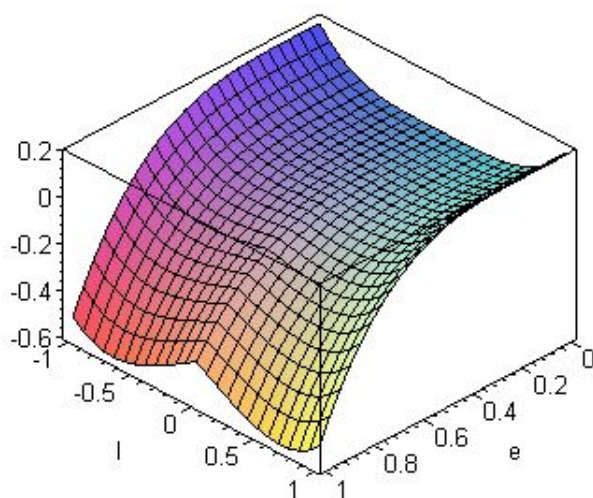
From the Equation (28), we see that the Weinhold scalar curvature of fluctuations vanishes identically. Namely, for all topological Einstein–Yang–Mills black holes, we find that the Weinhold scalar curvature vanishes identically and we have

$$R(e, l) = 0, \forall (e, l) \in \mathcal{M}_2 \tag{33}$$

It is surprising to notice that the topological Einstein–Yang–Mills black holes correspond to a non-interacting statistical system for $D > 5$. This follows from the vanishing value of the scalar curvature. In effect, we find it interesting that the scalar curvature vanishes identically for all values of the black hole parameters $\{e, l\}$. This shows that the fluctuating higher dimensional topological Einstein–Yang–Mills black holes are globally stability, namely, there are no vacuum phase transitions in the underlying ensemble. In short, the above consideration of the thermodynamic geometry indicates that

although the higher dimensional topological Einstein–Yang–Mills black holes are non-interacting in the global sense, they correspond to a stably vacuum configurations in a specific domain of the parameters. Namely, when the parameters $\{e, l\}$ are allowed to fluctuate, there exists certain domain of the $\{e, l\}$ in which there are positive set of the principle minors. Further, the above observation follows from the fact that there are non-trivial instabilities at the local level of the parametric fluctuations of the ensemble.

Figure 16. The determinant of the metric tensor plotted as the function of $\{e, l\}$, describing the fluctuations in six dimensional topological Einstein–Yang–Mills black hole configurations.



5. Conclusions

The thermodynamic geometric analysis of the topological Einstein–Yang–Mills black hole configurations is offered under the fluctuations of the vacuum parameters, namely the electric charge and the cosmological constant. Such fluctuations are expected to arise due to non-zero heating effects, chemical reactions and possible conventional vacuum fluctuation of a field theory configuration containing a background black hole. The intrinsic geometric method is used to examine the structures of the parametric fluctuations in an ensemble of arbitrary space-time dimension topological Einstein–Yang–Mills black holes. Thus, the stability analysis thus introduced is most generic for the fluctuations of the parameters that govern the quantum vacuum of the non-Abelian Yang–Mills gauge theory with a background black hole.

The present analysis is well suited for statistical selection of the stable vacua of the topological Einstein–Yang–Mills gauge theory. The thermodynamic geometric procedure is presented for the black holes carrying a (i) cosmological constant term and (ii) an electric charge. In this concern, the examination of the thermodynamic Ruppeiner and Weinhold geometries shows the entropy and energy flow properties respectively for an ensemble of Einstein–Yang–Mills black holes in $D > 5$. The local stability requires a set of positive heat capacities, while the global stability of the ensemble requires the positivity of the determinant of the metric tensor as well. These notions illustrate that the typical instability appears differently for the case of $D = 5$ and $D > 5$ topological Einstein–Yang–Mills black holes. Subsequently, it turns out that the associated ensembles of the topological Einstein–Yang–Mills

black holes correspond to a non-interacting system for $D = 5$, while it becomes ill-defined for the case of $D > 5$. From the perspective of the Weinhold geometry, the first case yields a nonzero scalar curvature, while the second case leads to a non-interacting statistical configuration. This follows from the fact that the manifold of parameters is curved, while it is flat the second case.

In the limit of the electric charge $e \in (0, 10)$ and cosmological parameter $l \in (-1, +1)$, we find that the determinant of the Ruppeiner metric tensor of the five dimensional topological Einstein–Yang–Mills black hole configurations remains positive, whereas the determinant of the Ruppeiner metric tensor of the six and higher dimensional topological Einstein–Yang–Mills black hole configurations vanishes identically for all values of the electric charge e and the cosmological parameter l . This shows that the five dimensional topological Einstein–Yang–Mills black hole can be statistically stabilized while the six and higher dimensional counterparts cannot. Thus, the present investigation predicts that the topological Einstein–Yang–Mills black hole systems with the fluctuating $\{e, l\}$ are relatively more stable for $D = 5$ and better-behaved than those in the $D > 5$. In addition, our model is well suited for the robust statistical examinations. Such black hole configurations are very known nowadays in string theory and M-theory vacuum solutions because of their existence in the low energy effective field theory configurations. From the viewpoint vacuum fluctuations, the parametric fluctuation theory offers a robust model that is very lucrative. It is worth mentioning that the use of the parametric geometric principle is rapidly growing in recent years in the area of black hole physics.

Based on the notion of the thermodynamic geometries, namely the definition of Ruppeiner geometry and Weinhold geometry, the thermodynamic stability analysis remains compatible for parametrically stable examinations of black holes and their ensemble properties. The present analysis thus provides the parametric geometric front to the stability analysis of the non-Abelian topological Yang–Mills black holes and their possible vacuum fluctuations. The method of the parametric geometry may be also used, in order to model in a suitable fashion the quantum part of the background fluctuations and the vacuum disturbances to the black hole background space-time configuration. Finally, it is expected that our analysis offers perspective stability grounds, when applied to the any finite parameter black hole in the Yang–Mills gauge theory. It is expected further that the present investigation would be an important factor in an appropriate examination of the statistical stability criteria of the required higher derivative corrections and the higher quantum loop corrections such that the considered black hole ensemble becomes statistically stable. This consideration can work as the indicator of fluctuations of the parameters of a given black hole ensemble, *i.e.*, whether it yields a statistically (in)stable quantum vacuum. Finally, it would be worth extending the present consideration of thermodynamic geometries for the dyonic Yang–Mills black holes and their embeddings in the gauged supergravities and string theories.

Acknowledgements

Supported in part by the European Research Council grant n. 226455, “*Supersymmetry, Quantum Gravity and Gauge Fields (SUPERFIELDS)*”. BNT thanks V. Ravishankar for support and encouragement towards the present research. BNT acknowledges the stimulating environments and local hospitality of (i) “*The Abdus Salam, International Centre for Theoretical Physics Trieste, Italy*”, during the “*Spring School on Superstring Theory and Related Topics (28 March 2011– 05 April 2011)*”;

(ii) “*The Galileo Galilei Institute for Theoretical Physics, Arcetri, Florence*”, during the “*Workshop on Large N Gauge Theories (02 May 2011–08 May 2011)*”; (iii) “*Les Houches School on Vicious Walkers and Random Martices, (16 May 2011–27 May 2011)*”, where a part of this research was presented in the Poster Session; and (iv) “*The Strings 2011, Uppsala Universitet, Sweden (27 June 2011–02 July 2011)*”, where a part of this research was presented in the Gong-show. The work of BNT has been supported by a postdoctoral research fellowship of “*INFN-Laboratori Nazionali di Frascati, Roma, Italy*”.

References

1. Ruppeiner, G. Riemannian geometry in thermodynamic fluctuation theory. *Rev. Mod. Phys.* **1995**, *67*, 605. Erratum **1996**, *68*, 313.
2. Ruppeiner, G. Thermodynamic curvature and phase transitions in Kerr–Newman black holes. *Phys. Rev. D* **2008**, *78*, 024016.
3. Ruppeiner, G. Thermodynamics: A Riemannian geometric model. *Phys. Rev. A* **1979**, *20*, 1608–1613.
4. Ruppeiner, G. Thermodynamic critical fluctuation theory? *Phys. Rev. Lett.* **1983**, *50*, 287–290.
5. Ruppeiner, G. New thermodynamic fluctuation theory using path integrals. *Phys. Rev. A* **1983**, *27*, 1116–1133.
6. Ruppeiner, G. Thermodynamic curvature of the multicomponent ideal gas. *Phys. Rev. A* **1990**, *41*, 2200–2202.
7. Tiwari, B.N. *On Generalized Uncertainty Principle*; LAP Academic Publication: Saarbrücken, Germany, 2011.
8. Tiwari, B.N. *Sur les corrections de la géométrie thermodynamique des trous noirs*; Éditions Universitaires Européennes: Saarbrücken, Germany, 2011.
9. Sarkar, T.; Sengupta, G.; Tiwari, B.N. On the thermodynamic geometry of BTZ black holes. *J. High Energ. Phys.* **2006**, *2006*, 15.
10. Sarkar, T.; Sengupta, G.; Tiwari, B.N. Thermodynamic geometry and extremal black holes in string theory. *J. High Energ. Phys.* **2008**, *2008*, 76.
11. Bellucci, S.; Tiwari, B.N. On the microscopic perspective of black branes thermodynamic geometry. *Entropy* **2010**, *12*, 2096.
12. Bellucci, S.; Tiwari, B.N. An exact fluctuating 1/2-BPS configuration. *J. High Energ. Phys.* **2010**, *2010*, 23.
13. Bellucci, S.; Tiwari, B.N. State-space correlations and stabilities. *Phys. Rev. D* **2010**, *82*, 084008.
14. Bellucci, S.; Tiwari, B.N. Thermodynamic geometry and Hawking radiation. *J. High Energ. Phys.* **2010**, *2010*, 30.
15. Bellucci, S.; Tiwari, B.N. Black strings, black rings and state-space manifold. *Int. J. Mod. Phys. A* **2011**, *26*, 5403–5464.
16. Bellucci, S.; Tiwari, B.N. State-space manifold and rotating black holes. *J. High Energ. Phys.* **2011**, *2011*, 118.
17. Aman, J.E.; Bengtsson, I.; Dokrajt, N. Flat information geometries in black hole thermodynamics. *Gen. Rel. Grav.* **2006**, *38*, 1305–1315.

18. Shen, J.; Cai, R.G.; Wang, B.; Su, R.K. Thermodynamic geometry and critical behavior of black holes. *Int. J. Mod. Phys. A* **2007**, *22*, 11–27.
19. Aman, J.E.; Bengtsson, I.; dokrajt, N. Geometry of black hole thermodynamics. *Gen. Rel. Grav.* **2003**, *35*, 1733–1743.
20. Aman, J.E.; Pidokrajt, N. Geometry of higher-dimensional black hole thermodynamics. *Phys. Rev. D* **2006**, *73*, 024017.
21. Tiwari, B.N. *Geometric Perspective of Entropy Function: Embeddings, Spectrum and Convexity*; LAP Academic Publication: Saarbrücken, Germany, 2011.
22. Weinhold, F. Metric geometry of equilibrium thermodynamics. *J. Chem. Phys.* **1975**, *63*, 2479–2484.
23. Weinhold, F. Metric geometry of equilibrium thermodynamics. II. Scaling, homogeneity, and generalized Gibbs–Duhem relations. *J. Chem. Phys.* **1975**, *63*, 2484–2488.
24. Bellucci, S.; Chandra, V.; Tiwari, B.N. On the thermodynamic geometry of hot QCD. *Int. J. Mod. Phys. A* **2011**, *26*, 43–70.
25. Bellucci, S.; Chandra, V.; Tiwari, B.N. A geometric approach to correlations and quark number susceptibilities. *Mod. Phys. Lett. A* **2010**, *27*, 10, 1250055–1250061.
26. Bellucci, S.; Chandra, V.; Tiwari, B.N. Thermodynamic stability of Quarkonium bound states. *Int. J. Mod. Phys. A* **2011**, *26*, 2665–2724.
27. Bartnik, R.; McKinnon, J. Particlelike solutions of the Einstein–Yang–Mills equations. *Phys. Rev. Lett.* **1988**, *61*, 141–144.
28. Yasskin, P.B. Solutions for gravity coupled to massless gauge fields. *Phys. Rev. D* **1975**, *12*, 2212–2217.
29. Winstanley, E. Physics of black holes. *Lect. Notes Phys.* **2009**, *769*, 49–87.
30. Okuyama, N.; Maeda, K. I. Five-dimensional black hole and particle solution with a non-Abelian gauge field. *Phys. Rev. D* **2003**, *67*, 104012–104030.
31. Mazharimousavi, S. H.; Halilsoy, M. Einstein–Yang–Mills black hole solution in higher dimensions by the Wu–Yang Ansatz. *Phys. Lett. B* **2008**, *659*, 471–475.
32. Brihaye, Y.; Chakrabarti, A.; Tchrakian, D.H. Particle-like solutions to higher-order curvature Einstein–Yang–Mills systems in d dimensions. *Classical Quant. Grav.* **2003**, *20*, 02765–02784.
33. Brihaye, Y.; Chakrabarti, A.; Hartmann, B.; Tchrakian, D.H. Higher order curvature generalizations of Bartnick–McKinnon and coloured black hole solutions in $d=5$. *Phys. Lett. B* **2003**, *561*, 161–173.
34. Torii, T.; Maeda, K.I., Tachizawa, T. Cosmic colored black holes. *Phys. Rev. D* **1995**, *52*, R4272–R4276.
35. Volkov, M. S.; Straumann, N.; Lavrelashvili, G.; Heusler, M.; Brodbeck, O. Cosmological analogues of the Bartnick–McKinnon solutions. *Phys. Rev. D* **1996**, *54*, 7243–7251.
36. Mann, R.B.; Radu, E.; Tchrakian, D.H. Non-Abelian solutions in AdS_4 and $d=11$ supergravity. *Phys. Rev. D* **2006**, *74*, 064015–064039.
37. Bjoraker, J.; Hosotani, Y.; Stable monopole and Dyon solutions in the Einstein–Yang–Mills theory in asymptotically anti-de Sitter space. *Phys. Rev. Lett.* **2000**, *84*, 1853–1856.

38. Baxter, J.E.; Winstanley, E. On the existence of soliton and hairy black hole solutions of $su(N)$ Einstein–Yang–Mills theory with a negative cosmological constant. *Classical Quant. Grav.* **2008**, *25*, 245014–245044.
39. Brodbeck, O.; Heusler, M.; Lavrelashvili, G.; Straumann, N.; Volkov, M.S. Stability analysis of new solutions of the EYM system with a cosmological constant. *Phys. Rev. D* **1996**, *54*, 7338–7352.
40. Winstanley, E. Existence of stable hairy black holes in $su(2)$ Einstein–Yang–Mills theory with a negative cosmological constant. *Classical Quant. Grav.* **1999**, *16*, 1963–1978.
41. Wu, T. T.; Yang, C.N. *Properties of Matter under Unusual Conditions*; Mark, H., Fenbarch, S., Eds.; Interscience: New York, NY, USA; 1969; pp. 349–354.
42. Bostani, N.; Dehghani, M.H. Topological black holes of $(n+1)$ -dimensional Einstein–Yang–Mills gravity. *Mod. Phys. Letts. A* **2010**, *25*, 18, 1507–1519.
43. Cvetič, M.; Lu, H.; Pope, C.N. Non-Abelian black holes in $D=5$ maximal gauged supergravity. *Phys. Rev. D* **2010**, *81*, 044023–044030.
44. Hubeny, V.E.; Minwalla, S.; Rangamani, M. The fluid/gravity correspondence. *arXiv* **2011**, arXiv:1107.5780v1.
45. Banerjee, N.; Bhattacharya, J.; Bhattacharyya, S.; Jain, S.; Minwalla, S.; Sharma, T. Constraints on fluid dynamics from equilibrium partition functions. *arXiv* **2012**, arXiv:1203.3544v1.

Appendix A: Ruppeiner Geometry of Higher Dimensional Topological Einstein–Yang–Mills Black Holes

In this appendix, we provide the specific factors of the Christoffel symbols of the state-space Ruppeiner geometry of arbitrary topological Einstein–Yang–Mills black hole configuration. Namely, we find after simplification of the Equation (18) that the factors $\{\Gamma_{ijk}^{(l)}\}$ are given as per the followings

$$\begin{aligned}
 \Gamma_{eee}^{(1)} &= 16e^4n^3 - 48n^2e^4 + 4e^2n^3l^2 - 8l^2n^2e^2 \\
 &\quad - 12l^2ne^2 + 3l^4n^2 - 18l^4n + 24l^4 \\
 \Gamma_{eee}^{(2)} &= +3l^4n^2 - 18l^4n + 24l^4 \\
 \Gamma_{eel}^{(1)} &= 32e^6n^4 - 64e^6n^3 + 8e^4n^4l^2 - 48e^4l^2n^2 \\
 &\quad + 8e^2n^3l^4 - 38e^2l^4n^2 + 44e^2l^4n + l^6n^2 \\
 &\quad - 4nl^6 + 4l^6 \\
 \Gamma_{eel}^{(2)} &= 8l^2n^3e^4 - 16e^4n^2l^2 + 8l^4n^3e^2 - 40l^4n^2e^2 \\
 &\quad + 48l^4ne^2 + l^6n^2 - 4l^6n + 4l^6 \\
 \Gamma_{ele}^{(1)} &= 32e^6n^4 - 64e^6n^3 + 8e^4n^4l^2 - 48e^4l^2n^2 \\
 &\quad + 8e^2n^3l^4 - 38e^2l^4n^2 + 44e^2l^4n + l^6n^2 \\
 &\quad - 4nl^6 + 4l^6 \\
 \Gamma_{ele}^{(2)} &= 8l^2n^3e^4 - 16e^4n^2l^2 + 8l^4n^3e^2 - 40l^4n^2e^2 \\
 &\quad + 48l^4ne^2 + l^6n^2 - 4l^6n + 4l^6
 \end{aligned}$$

$$\begin{aligned}
\Gamma_{ell}^{(1)} &= 16e^6 n^4 - 16e^6 n^3 + 4e^4 n^4 l^2 + 8e^4 n^3 l^2 \\
&\quad - 36e^4 l^2 n^2 + 5e^2 n^3 l^4 - 20e^2 l^4 n^2 + 20e^2 l^4 n \\
&\quad + l^6 n^2 - 4nl^6 + 4l^6 \\
\Gamma_{ell}^{(2)} &= 8l^2 n^3 e^4 - 16e^4 n^2 l^2 + 5l^4 n^3 e^2 - 22l^4 n^2 e^2 \\
&\quad + 24l^4 n e^2 + l^6 n^2 - 4l^6 n + 4l^6 \\
\Gamma_{lle}^{(1)} &= 16e^6 n^4 - 16e^6 n^3 + 4e^4 n^4 l^2 + 8e^4 n^3 l^2 \\
&\quad - 36e^4 l^2 n^2 + 20e^2 l^4 n + l^6 n^2 - 4nl^6 \\
&\quad + 4l^6 + 5e^2 n^3 l^4 - 20e^2 l^4 n^2 \\
\Gamma_{lle}^{(2)} &= 8l^2 n^3 e^4 - 16e^4 n^2 l^2 + 5l^4 n^3 e^2 - 22l^4 n^2 e^2 \\
&\quad + 24l^4 n e^2 + l^6 n^2 - 4l^6 n + 4l^6 \\
\Gamma_{lll}^{(1)} &= 32e^6 n^4 + 8e^4 n^4 l^2 + 32e^4 n^3 l^2 - 96e^4 l^2 n^2 \\
&\quad + 12e^2 n^3 l^4 - 42e^2 l^4 n^2 + 36e^2 l^4 n + 3l^6 n^2 \\
&\quad - 12nl^6 + 12l^6 \\
\Gamma_{lll}^{(2)} &= 24l^2 n^3 e^4 - 48e^4 n^2 l^2 + 12l^4 n^3 e^2 - 48l^4 n^2 e^2 \\
&\quad + 48l^4 n e^2 + 3l^6 n^2 - 12l^6 n + 12l^6
\end{aligned} \tag{34}$$

Appendix B: Weinhold Geometry of Five Dimensional Topological Einstein–Yang–Mills Black Holes

In this appendix, we provide the specific quantities for the Weinhold geometry of five dimensional topological Einstein–Yang–Mills black holes. Namely, for the determinant of the metric tensor, as given in the Equation (24), we find that the factors $\{r_i(l)\}$ can be written as the following expressions

$$\begin{aligned}
r_0 &= (2 \ln(lb) - 4 \ln(2) - 1)l^5 + 4(3 \ln(lb) - 6 \ln(2) - 1)l^6 \\
&\quad + 24(\ln(lb) - 2 \ln(2))l^7 + 2(10 \ln(lb) - 20 \ln(2) + 7)l^8 \\
&\quad + (6 \ln(lb) - 12 \ln(2) + 17)l^9 + 6l^{10} \\
r_1 &= -8(2 \ln(lb) - 4 \ln(2) + 7)l^3 - 256l^4 + 4(46 \ln(lb) - 92 \ln(2) - 67)l^5 \\
&\quad + 4(78 \ln(lb) - 156 \ln(2) + 35)l^6 + 16(9 \ln(lb) - 18 \ln(2) + 21)l^7 \\
&\quad + 128l^8 \\
r_2 &= -256(\ln(lb) - 2 \ln(2) + 4)l^2 - 2560l^3 \\
&\quad + 32(42 \ln(lb) - 84 \ln(2) - 19)l^4 + 128(9 \ln(lb) - 18 \ln(2) + 14)l^5 \\
&\quad + 768l^6 \\
r_3 &= -256(6l \ln(lb) - 12l \ln(2) + 25)l + 256(2 \ln(lb) - 4l^2 \ln(2) - 35)l^2 \\
&\quad + 1024(3 \ln(lb) - 6l^3 \ln(2) - 1)l^3 \\
r_4 &= -18432 + 8192 \ln(2) - 20480l - 4096 \ln(lb) - 8192l^2
\end{aligned} \tag{35}$$

From the viewpoint of the global chemical fluctuations, we find that the factors in the numerator of the Weinhold scalar curvature as given by the Equation (25) can be expressed as

$$\begin{aligned}
R_0 &= -8l^8 + (12\tilde{b} - 24\ln(2) - 94)l^9 + (84\tilde{b} - 168\ln(2) - 438)l^{10} \\
&\quad + (246\tilde{b} - 492\ln(2) - 1087)l^{11} + (390\tilde{b} - 780\ln(2) - 1591)l^{12} \\
&\quad + (360\tilde{b} - 720\ln(2) - 1412)l^{13} + (192\tilde{b} - 384\ln(2) - 740)l^{14} \\
&\quad + (54\tilde{b} - 108\ln(2) - 207)l^{15} + (6\tilde{b} - 12\ln(2) - 23)l^{16} \\
R_1 &= -64l^6 + (64\tilde{b} - 128\ln(2) - 928)l^7 + (576\tilde{b} - 1152\ln(2) - 5728)l^8 \\
&\quad + (2304\tilde{b} - 4608\ln(2) - 17984)l^9 + (5008\tilde{b} - 10016\ln(2) - 31976)l^{10} \\
&\quad + (6288\tilde{b} - 12576\ln(2) - 33560)l^{11} + (4560\tilde{b} - 9120\ln(2) - 20448)l^{12} \\
&\quad + (1776\tilde{b} - 3552\ln(2) - 6584)l^{13} + (288\tilde{b} - 576\ln(2) - 840)l^{14} \\
R_2 &= (512\ln(2) - 256\tilde{b} - 3456)l^5 + (768\tilde{b} - 1536\ln(2) - 27776)l^6 \\
&\quad + (8704\tilde{b} - 17408\ln(2) - 107776)l^7 + (26880\tilde{b} - 53760\ln(2) - 237952)l^8 \\
&\quad + (45312\tilde{b} - 90624\ln(2) - 306432)l^9 + (45312\tilde{b} - 90624\ln(2) - 224128)l^{10} \\
&\quad + (24960\tilde{b} - 49920\ln(2) - 84672)l^{11} + (5760\tilde{b} - 11520\ln(2) - 12480)l^{12} \\
R_3 &= +(8192\ln(2) - 4096\tilde{b} - 55296)l^4 + (12288\tilde{b} - 24576\ln(2) - 321536)l^5 \\
&\quad + (98304\tilde{b} - 196608\ln(2) - 892928)l^6 + (221184\tilde{b} - 442368\ln(2) - 1427456)l^7 \\
&\quad + (276480\tilde{b} - 552960\ln(2) - 1281536)l^8 + (199680\tilde{b} - 399360\ln(2) - 574976)l^9 \\
&\quad + (61440\tilde{b} - 122880\ln(2) - 96768)l^{10} \\
R_4 &= (49152\ln(2) - 24576\tilde{b} - 430080)l^3 + (155648\tilde{b} - 311296\ln(2) - 1945600)l^4 \\
&\quad + (737280\tilde{b} - 1474560\ln(2) - 3956736)l^5 + (1179648\tilde{b} - 2359296\ln(2) - 4325376)l^6 \\
&\quad + (991232\tilde{b} - 1982464\ln(2) - 2281472)l^7 + (368640\tilde{b} - 737280\ln(2) - 413696)l^8 \\
R_5 &= +(131072\ln(2) - 65536\tilde{b} - 1933312)l^2 + (983040\tilde{b} - 1966080\ln(2) - 6586368)l^3 \\
&\quad + (2949120\tilde{b} - 5898240\ln(2) - 8978432)l^4 + (2949120\tilde{b} - 5898240\ln(2) - 5406720)l^5 \\
&\quad + (1179648\tilde{b} - 2359296\ln(2) - 884736)l^6 \\
R_6 &= -4718592l + (3145728\tilde{b} - 629145\ln(2) - 9961472)l^2 \\
&\quad + (4718592\tilde{b} - 9437184\ln(2) - 6553600)l^3 + (1572864\tilde{b} - 3145728\ln(2) - 262144)l^4 \\
R_7 &= -6291456 + (4194304\tilde{b} - 8388608\ln(2) - 2097152)l + 2097152l^2 \tag{36}
\end{aligned}$$

Appendix C: Weinhold Geometry of Higher Dimensional Topological Einstein–Yang–Mills Black Holes

In this appendix, we offer the explicit expressions for the Weinhold geometry of arbitrary higher dimensional topological Einstein–Yang–Mills black holes of fluctuations. From the definition of the chemical geometry, we find that the factors $\{\Gamma_{ijk}^{(1)}, \Gamma_{ijk}^{(2)} | i, j, k \in \{e, l\}\}$ of the Christoffel symbols as given in Equation (30) can be expressed as the following set of the equations

$$\begin{aligned}
 \Gamma_{eee}^{(1)} &= 4n^2 e^4 + n^2 e^2 l^2 + 8n e^2 l^2 + 3l^4 n - 6l^4 \\
 \Gamma_{eee}^{(2)} &= e^2 l^2 n^2 + 2e^2 l^2 n + 3l^4 n - 6l^4 \\
 \Gamma_{eel}^{(1)} &= e^2 l^6 n^3 + e^2 n^4 l^6 + 20e^2 l^6 n - 16e^2 l^6 n^2 \\
 &\quad + 4e^4 l^4 n^2 - 18e^4 l^4 n^3 + 8e^4 n^4 l^4 - 31e^6 l^2 n^3 \\
 &\quad + 19e^6 n^4 l^2 - 8l^8 + n^3 l^8 + 12n^4 e^8 - 6n^2 l^8 \\
 &\quad + 12l^8 n \\
 \Gamma_{eel}^{(2)} &= 2n^4 e^8 + 12l^8 n - 6l^8 n^2 + l^8 n^3 \\
 &\quad + l^6 n^4 e^2 - l^6 n^3 e^2 - 17l^2 n^3 e^6 + 12l^4 n^2 e^4 \\
 &\quad + 9l^2 n^4 e^6 - 18l^4 n^3 e^4 - 8l^6 n^2 e^2 + 12l^6 n e^2 \\
 &\quad + 6l^4 n^4 e^4 - 8l^8 \\
 \Gamma_{ele}^{(1)} &= e^2 l^6 n^3 + e^2 n^4 l^6 + 20e^2 l^6 n - 16e^2 l^6 n^2 \\
 &\quad + 4e^4 l^4 n^2 - 18e^4 l^4 n^3 + 8e^4 n^4 l^4 - 31e^6 l^2 n^3 \\
 &\quad + 19e^6 n^4 l^2 - 8l^8 + n^3 l^8 + 12n^4 e^8 \\
 &\quad - 6n^2 l^8 + 12l^8 n \\
 \Gamma_{ele}^{(2)} &= 2n^4 e^8 + 12l^8 n - 6l^8 n^2 + l^8 n^3 \\
 &\quad + l^6 n^4 e^2 - l^6 n^3 e^2 - 17l^2 n^3 e^6 + 12l^4 n^2 e^4 \\
 &\quad + 9l^2 n^4 e^6 - 18l^4 n^3 e^4 - 8l^6 n^2 e^2 + 12l^6 n e^2 \\
 &\quad + 6l^4 n^4 e^4 - 8l^8 \\
 \Gamma_{ell}^{(1)} &= l^8 n^5 + 9e^2 n^5 l^6 + 26e^4 n^5 l^4 + 25e^6 n^5 l^2 \\
 &\quad - 13l^8 n^4 + 372e^2 l^6 n^3 - 98e^2 n^4 l^6 + 352e^2 l^6 n \\
 &\quad - 600e^2 l^6 n^2 - 508e^4 l^4 n^2 + 612e^4 l^4 n^3 + 4n^5 e^8 \\
 &\quad - 231e^4 n^4 l^4 + 256e^6 l^2 n^3 - 178e^6 n^4 l^2 - 80l^8 \\
 &\quad + 64n^3 l^8 - 24n^4 e^8 - 152n^2 l^8 + 176l^8 n \\
 \Gamma_{ell}^{(2)} &= +l^8 n^5 - 13l^8 n^4 + 176l^8 n - 152l^8 n^2 \\
 &\quad + 64l^8 n^3 + 7l^2 n^5 e^6 + 14l^4 n^5 e^4 + 7l^6 n^5 e^2 \\
 &\quad - 76l^6 n^4 e^2 + 288l^6 n^3 e^2 + 76l^2 n^3 e^6 - 276l^4 n^2 e^4 \\
 &\quad - 52l^2 n^4 e^6 + 332l^4 n^3 e^4 - 464l^6 n^2 e^2 + 272l^6 n e^2 \\
 &\quad - 125l^4 n^4 e^4 - 80l^8
 \end{aligned}$$

$$\begin{aligned}
\Gamma_{le}^{(1)} &= l^8 n^5 + 10 e^2 n^5 l^6 + 34 e^4 n^5 l^4 + 44 e^6 n^5 l^2 \\
&\quad - 13 l^8 n^4 + 414 e^2 l^6 n^3 - 109 e^2 n^4 l^6 + 392 e^2 l^6 n \\
&\quad - 668 e^2 l^6 n^2 - 664 e^4 l^4 n^2 + 800 e^4 l^4 n^3 - 302 e^4 n^4 l^4 \\
&\quad + 442 e^6 l^2 n^3 - 309 e^6 n^4 l^2 + 16 n^5 e^8 - 80 l^8 \\
&\quad + 64 n^3 l^8 - 88 n^4 e^8 - 152 n^2 l^8 + 176 l^8 n \\
\Gamma_{le}^{(2)} &= 2 n^5 e^8 l^2 - 13 l^8 n^4 + l^8 n^5 - 12 n^4 e^8 \\
&\quad + 176 l^8 n - 152 l^8 n^2 + 64 l^8 n^3 + 16 l^2 n^5 e^6 \\
&\quad + 20 l^4 n^5 e^4 + 8 l^6 n^5 e^2 - 87 l^6 n^4 e^2 + 330 l^6 n^3 e^2 \\
&\quad + 166 l^2 n^3 e^6 - 392 l^4 n^2 e^4 - 115 l^2 n^4 e^6 + 472 l^4 n^3 e^4 \\
&\quad - 532 l^6 n^2 e^2 + 312 l^6 n e^2 - 178 l^4 n^4 e^4 - 80 l^8 \\
\Gamma_{ll}^{(1)} &= 3360 n^5 e^4 l^6 - 8768 n^4 e^6 l^4 + n^7 l^{10} + 192 n^5 e^{10} + 4404 n^5 e^6 l^4 \\
&\quad + 41 n^7 e^8 l^2 - 384 l^{10} - 530 n^6 e^8 l^2 - 6304 n^2 e^2 l^8 + 11728 n^3 e^4 l^6 \\
&\quad - 924 n^6 e^6 l^4 + 6544 n^3 e^2 l^8 - 9008 n^4 e^4 l^6 + 1076 n^5 e^2 l^8 \\
&\quad + 43 n^7 e^4 l^6 - 608 n^6 e^4 l^6 - 3568 n^4 e^2 l^8 + 70 n^7 e^6 l^4 \\
&\quad - 1552 l^{10} n^2 - 17 l^{10} n^6 + 122 l^{10} n^5 - 480 l^{10} n^4 \\
&\quad + 1120 l^{10} n^3 + 1184 l^{10} n - 56 n^6 e^{10} + 4 n^7 e^{10} \\
&\quad + 2144 n^5 e^8 l^2 + 11 n^7 e^2 l^8 - 170 n^6 e^2 l^8 + 2496 l^8 e^2 n \\
&\quad + 6192 l^4 e^6 n^3 - 5952 l^6 e^4 n^2 - 2496 l^2 n^4 e^8 \\
\Gamma_{ll}^{(2)} &= 1184 l^{10} n + 1120 l^{10} n^3 - 384 l^{10} - 480 l^{10} n^4 \\
&\quad - 1552 l^{10} n^2 - 17 l^{10} n^6 + 122 l^{10} n^5 + l^{10} n^7 \\
&\quad - 5976 l^6 n^4 e^4 + 9 n^7 e^8 l^2 + 556 n^5 e^8 l^2 + 2060 l^4 n^5 e^6 \\
&\quad - 4208 l^4 n^4 e^6 - 5312 l^8 n^2 e^2 + 5488 l^8 n^3 e^2 + 7872 l^6 n^3 e^4 \\
&\quad + 2112 l^8 n e^2 - 4032 l^6 n^2 e^4 + 3024 l^4 n^3 e^6 + 2196 l^6 n^5 e^4 \\
&\quad + 30 n^7 e^6 l^4 - 128 n^6 e^8 l^2 - 390 l^6 n^6 e^4 + 27 l^6 n^7 e^4 \\
&\quad - 672 n^4 e^8 l^2 + 892 l^8 n^5 e^2 - 140 n^6 e^2 l^8 + 9 n^7 e^2 l^8 \\
&\quad - 416 n^6 e^6 l^4 - 2976 l^8 n^4 e^2
\end{aligned} \tag{37}$$

From the characterization of the global fluctuation properties, we find that the factors $\{g_{li} \mid i = 1, \dots, 10\}$ of degree 20 of the determinant of the metric tensor as given in the Equation (31) can be written as per the following expressions

$$\begin{aligned}
g_{10} &= -3145728 + 16777216 n - 40632320 n^2 + 58982400 n^3 - 57016320 n^4 \\
&\quad + 38535168 n^5 - 18579456 n^6 + 6389760 n^7 - 1536000 n^8 + 245760 n^9 \\
&\quad - 23552 n^{10} + 1024 n^{11}
\end{aligned}$$

$$\begin{aligned}
g_{11} &= 40894464 n - 197656576 n^2 + 429391872 n^3 - 552075264 n^4 + 465174528 n^5 \\
&\quad - 268369920 n^6 + 107347968 n^7 - 29392896 n^8 + 5271552 n^9 - 559104 n^{10} \\
&\quad + 26624 n^{11} \\
g_{12} &= -225705984 n^2 + 978059264 n^3 - 1880883200 n^4 + 2106589184 n^5 \\
&\quad - 1514110976 n^6 + 724140032 n^7 - 230408192 n^8 + 47022080 n^9 \\
&\quad - 5583872 n^{10} + 293888 n^{11} \\
g_{13} &= 680263680 n^3 - 2607677440 n^4 + 4365025280 n^5 - 4166615040 n^6 \\
&\quad + 2480128000 n^7 - 942448640 n^8 + 223211520 n^9 - 30115840 n^{10} \\
&\quad + 1771520 n^{11} \\
g_{14} &= -1184563200 n^4 + 3948544000 n^5 - 5626675200 n^6 + 4442112000 n^7 \\
&\quad - 2097664000 n^8 + 592281600 n^9 - 92544000 n^{10} + 6169600 n^{11} \\
g_{15} &= 1109065728 n^5 - 3142352896 n^6 + 3696885760 n^7 - 2310553600 n^8 \\
&\quad + 808693760 n^9 - 150185984 n^{10} + 11552768 n^{11} \\
g_{16} &= -307888128 n^6 + 718405632 n^7 - 667090944 n^8 + 307888128 n^9 \\
&\quad - 70557696 n^{10} + 6414336 n^{11} \\
g_{17} &= -382205952 n^7 + 700710912 n^8 - 477757440 n^9 + 143327232 n^{10} \\
&\quad - 15925248 n^{11} \\
g_{18} &= 377487360 n^8 - 503316480 n^9 + 220200960 n^{10} - 31457280 n^{11} \\
g_{19} &= -110100480 n^9 + 91750400 n^{10} - 18350080 n^{11} \\
g_{110} &= 6291456 n^{10} - 2097152 n^{11}
\end{aligned} \tag{38}$$

Similarly, it follows that the factors $\{g_{2i} \mid i = 1, \dots, 9\}$ of degree 18 of the determinant of metric tensor as defined in the Equation (31) are given by

$$\begin{aligned}
g_{20} &:= -3145728 + 16777216 n - 40632320 n^2 + 58982400 n^3 - 57016320 n^4 \\
&\quad + 38535168 n^5 - 18579456 n^6 + 6389760 n^7 - 1536000 n^8 + 245760 n^9 \\
&\quad - 23552 n^{10} + 1024 n^{11} \\
g_{21} &:= 37748736 n - 182452224 n^2 + 396361728 n^3 - 509607936 n^4 + 429391872 n^5 \\
&\quad - 247726080 n^6 + 99090432 n^7 - 27131904 n^8 + 4866048 n^9 - 516096 n^{10} \\
&\quad + 24576 n^{11} \\
g_{22} &:= -189530112 n^2 + 821297152 n^3 - 1579417600 n^4 + 1768947712 n^5 \\
&\quad - 1271431168 n^6 + 608075776 n^7 - 193478656 n^8 + 39485440 n^9 \\
&\quad - 4688896 n^{10} + 246784 n^{11} \\
g_{23} &:= 508035072 n^3 - 1947467776 n^4 + 3259891712 n^5 - 3111714816 n^6 \\
&\quad + 1852211200 n^7 - 703840256 n^8 + 166699008 n^9 - 22491136 n^{10} \\
&\quad + 1323008 n^{11}
\end{aligned}$$

$$\begin{aligned}
g_{24} &:= -754384896 n^4 + 2514616320 n^5 - 3583328256 n^6 + 2828943360 n^7 \\
&\quad - 1335889920 n^8 + 377192448 n^9 - 58936320 n^{10} + 3929088 n^{11} \\
g_{25} &:= 534773760 n^5 - 1515192320 n^6 + 1782579200 n^7 - 1114112000 n^8 \\
&\quad + 389939200 n^9 - 72417280 n^{10} + 5570560 n^{11} \\
g_{26} &:= 14155776 n^6 - 33030144 n^7 + 30670848 n^8 - 14155776 n^9 \\
&\quad + 3244032 n^{10} - 294912 n^{11}, \\
g_{27} &:= -283115520 n^7 + 519045120 n^8 - 353894400 n^9 + 106168320 n^{10} \\
&\quad - 11796480 n^{11} \\
g_{28} &:= 160432128 n^8 - 213909504 n^9 + 93585408 n^{10} - 13369344 n^{11} \\
g_{29} &:= -25165824 n^9 + 20971520 n^{10} - 4194304 n^{11}
\end{aligned} \tag{39}$$

© 2012 by the authors; licensee MDPI, Basel, Switzerland. This article is an open access article distributed under the terms and conditions of the Creative Commons Attribution license (<http://creativecommons.org/licenses/by/3.0/>).